Research Paper

GEOSPHERE

GEOSPHERE

https://doi.org/10.1130/GES02405.1

13 figures; 5 tables; 1 set of supplemental files

CORRESPONDENCE: gav4@buffalo.edu

CITATION: Valentine, G.A., Ort, M.H., and Cortés, J.A., 2021, Quaternary basaltic volcanic fields of the American Southwest: Geosphere, https://doi.org/10.1130/GES02405.1.

Science Editor: Shanaka de Silva

Received 22 January 2021
Revision received 21 April 2021
Accepted 25 June 2021

Published online 2 November 2021

Quaternary basaltic volcanic fields of the American Southwest

Greg A. Valentine[1], Michael H. Ort[2], and Joaquín A. Cortés[3]

[1]Department of Geology and Center for Geohazards Studies, University at Buffalo, 126 Cooke Hall, Buffalo, New York 14260, USA
[2]School of Earth and Sustainability, P.O. Box 4099, Northern Arizona University, Flagstaff, Arizona 86011, USA
[3]Department of Geography and Geology, Edge Hill University, St. Helens Road, Ormskirk, Lancashire L39 4QP, UK

ABSTRACT

The southwestern United States contains numerous monogenetic basaltic volcanoes distributed in intraplate volcanic fields. We review, on a regional scale, our current understanding of the Quaternary basalts with a focus on aspects pertinent to hazard assessment, such as physical volcanology and geochronology, while also summarizing the several petrogenetic conceptual models that have been proposed for the range of local tectonic settings in the region. We count 2229 volcanoes in 37 volcanic fields (including the Pinacate volcanic field, which is mostly in northern Sonora, Mexico). Volcanic landforms are dominantly scoria cones and ramparts with attendant lava fields that have a spectrum of 'a'ā and blocky to pāhoehoe morphologies, while a small percentage of the volcanoes are maars and tuff cones. Explosive eruption styles that were driven mainly by magmatic volatiles, where they have been studied in detail, included Hawaiian, Strombolian, violent Strombolian, and sub-Plinian activity. The latter two have resulted in substantial fallout deposits that can be traced tens of kilometers from source vents. Phreatomagmatic styles have produced pyroclastic current (mainly pyroclastic surges), ballistic, and fallout deposits. These eruption styles pose hazards to humans when they occur in populated areas and to air travel and regional infrastructure even in sparsely populated areas. All but one of the major volcanic fields (fields that contain ~100 or more Quaternary volcanoes) together form a northwest-southeast–trending band, which we suggest may reflect an influence of plate-boundary-related shearing on melt segregation in the upper mantle along with other factors; this view is consistent with recent global positioning system (GPS) and structural geologic data indicating the influence of dextral motion along the North America-Pacific plate boundary deep inside the Southwest. Of the 2229 Quaternary volcanoes identified, ~548 (25%) have been dated, and only ~15% have been dated with methods such as $^{40}Ar/^{39}Ar$ and cosmogenic surface exposure methods that are considered optimal for young basalts. Acknowledging the large uncertainty due to the poor geochronological data coverage, we use a simple Poisson model to provide a first-order estimate of recurrence rates of monogenetic volcanoes on the scale of the region as a whole; recurrence rates using our compiled age data set range from 3.74×10^{-4} yr^{-1} to 8.63×10^{-4} yr^{-1}. These values are only based on dated and mapped volcanoes, respectively, and do not account for undated and buried volcanoes or other uncertainties in the volcano count. The time between monogenetic eruptions in the Southwest is similar to the repose times of some polygenetic volcanoes, which suggests that the regional hazard is potentially commensurate with the hazard from a reawakening stratovolcano such as those in the Cascade Range. Notable in our review is that only a few volcanoes have been the subject of physical volcanological characterization, interpretation, and detailed petrologic study that may elucidate factors such as magma generation, ascent (including time scales), and controls on eruption style.

Greg Valentine https://orcid.org/0000-0002-8133-5878

INTRODUCTION AND BACKGROUND

The southwestern United States—here simply referred to as the Southwest—is dotted with volcanic fields composed mainly of basaltic, small-volume (<1 km^3) volcanoes. Most of these fields have been the subjects of geochemical and petrologic studies in varying levels of detail to better understand magma genesis in the dominantly extensional to neutral, intraplate tectonic settings of the region. Until recently, less research had focused on the interpretation of eruptive processes based upon their landforms, lavas, and pyroclastic products; the many scoria cones were simply assumed to record Strombolian eruptions, while maars and tuff cones record explosive magma-water interaction. Research during the past 15 years has shown, instead, that the volcanoes provide a rich record of eruptive processes and controlling factors (e.g., Genareau et al., 2010; Valentine et al., 2017; Alfano et al., 2019). The small size and relative simplicity of the individual basaltic volcanoes scattered within the fields, compared to composite and shield volcanoes, for example, facilitates research focused on specific processes without having to filter out some of the complexities of the larger and longer-lived systems. Volcanic fields are also referred to as distributed volcanism to distinguish them from central volcanoes (shields, composite volcanoes; see Smith and Németh, 2017, for additional discussion of the differences in these types of systems).

Southwestern basaltic volcanoes traditionally were not the subject of extensive hazard and risk assessment; they were assumed—at least implicitly—to not pose a threat. However, physical volcanological studies, partly motivated by interest in the impact of eruptions on pre-Columbian cultures (Ort et al., 2008a, 2008b) and by volcanic hazard assessment for the proposed Yucca Mountain radioactive waste repository (Valentine and Perry,

TABLE 1. HAZARDS ASSOCIATED WITH MONOGENETIC BASALTIC VOLCANOES

Eruption style	Volcanic process	Damage mechanism
Magmatic[1]		
Lava effusion	Lava flows	Inundation, topography modification (lava fields).
Strombolian	Lava fountains, cone building	Ballistic bombs, gasses and dilute ash plumes, topography modification (cone).
Violent Strombolian to sub-Plinian	Sustained eruption column, cone building	Ash plume, weight from tephra deposits, perturbed surface hydrologic and sediment transport processes, ballistic blocks and bombs, topography modification (cone and tephra sheet).
Phreatomagmatic[2]		
Maar or tuff ring forming	Pyroclastic density currents, crater development, tephra column	Temperature and dynamic pressure of density currents, weight from tephra deposits, ash plume, perturbed surface hydrologic and sediment transport processes, ballistic blocks and bombs, topography modification (crater excavation and subsidence, tephra ring, tephra sheet).
Tuff cone forming	Pyroclastic density currents, wet tephra column, cone building	Temperature and dynamic pressure of density currents, weight from tephra deposits, ash plume, perturbed surface hydrologic and sediment transport processes, ballistic blocks and bombs, topography modification (cone and tephra sheet).
Secondary hazards triggered by eruptions		
Fire, surface water drainage reorganization, flooding and debris flows, crop and livestock damage		

[1]Magmatic eruption processes are driven primarily by the expansion of magmatic volatiles (see Valentine and Gregg, 2008).
[2]Phreatomagmatic eruption processes are driven primarily by explosive interaction between magma and externally derived water (groundwater or surface water; see White and Ross, 2011).

2009), showed that, in addition to explosive phreatomagmatic eruptions, some basaltic monogenetic eruptions in the region included phases of violent Strombolian to sub-Plinian intensity that produced tephra-laden plumes approaching altitudes of 20 km (Alfano et al., 2019). Most intraplate volcanoes in the Southwest are in sparsely populated areas, and eruptions therefore may present lower threat to human life on the ground (although populations are locally increasing) than those in more densely populated volcanic regions. However, a violent Strombolian, sub-Plinian, or phreatomagmatic eruption could severely impact national air traffic as well as regional energy, transportation, and communication infrastructure. Other eruptive processes could pose hazards as well (Table 1).

We briefly review the literature on volcanic fields of the Southwest (here defined as the region between 31°N and 42°N and 103°W and 120°W), including geochronology, physical volcanology, and locations of basaltic volcanoes in the eight most active fields in the United States and one field in the Mexican state of Sonora that overlaps the Mexico-U.S. border (Fig. 1; Table 2). Basaltic volcanism started in the region during Miocene times (Christiansen and Lipman, 1972; Smith and Luedke, 1984), but we emphasize the Quaternary record (2.58 Ma to present) because it is both more relevant to future activity and because the volcanic record is better preserved. To focus on the more typical intraplate activity, we do not consider volcanic fields associated with the southern Cascades arc (northern California), the Snake River Plain area—which is related to the Yellowstone hot spot (Rivera et al., 2021)—nor the Salton Sea area of southern California, which contains only small-volume rhyolite domes and is related to a developing sea-floor spreading center (Gulf of California; Schmitt and Hulen, 2008). The review includes a compilation of all readily available age dates for Quaternary basalts in the region (Table S1[1], Supplemental Material), which we use to compute an initial estimate of the annual recurrence rate from Quaternary volcanic fields on the scale of the entire region. To our knowledge, this is the first broad compilation of the state of knowledge of distributed Quaternary, basaltic volcanism of the southwestern United States. We hope that our work can motivate future studies to remediate the large gaps in our knowledge of distributed volcanism; these gaps include basic geochronology, physical volcanology, and more detailed petrogenetic research.

TERMS AND APPROACH

Terms

We use the term basaltic loosely to include basalts sensu stricto, alkali basalts, trachybasalts, basaltic andesites (or basaltic trachyandesites), tephrites, and basanites. We follow Valentine and Connor (2015) in defining a volcano as *monogenetic* if it has one eruptive episode and is then extinct. As with a larger polygenetic volcano, an eruptive episode can have a duration of hours to decades (perhaps on the order of a century in some cases) and involve many styles of eruptive activity as well as waxing, waning, and quiescent cycles. This definition does not imply a "simple eruption," nor does it imply a single or simple magma composition or origin. As reviewed by McGee and Smith (2016), monogenetic volcanoes can experience varying degrees of magma evolution

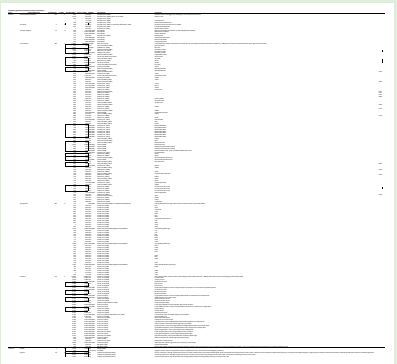

[1]Supplemental Material. Listing of published age dates and total Quaternary volcano counts in the southwest USA. Please visit https://doi.org/10.1130/GEOS.S.15175932 to access the supplemental material, and contact editing@geosociety.org with any questions.

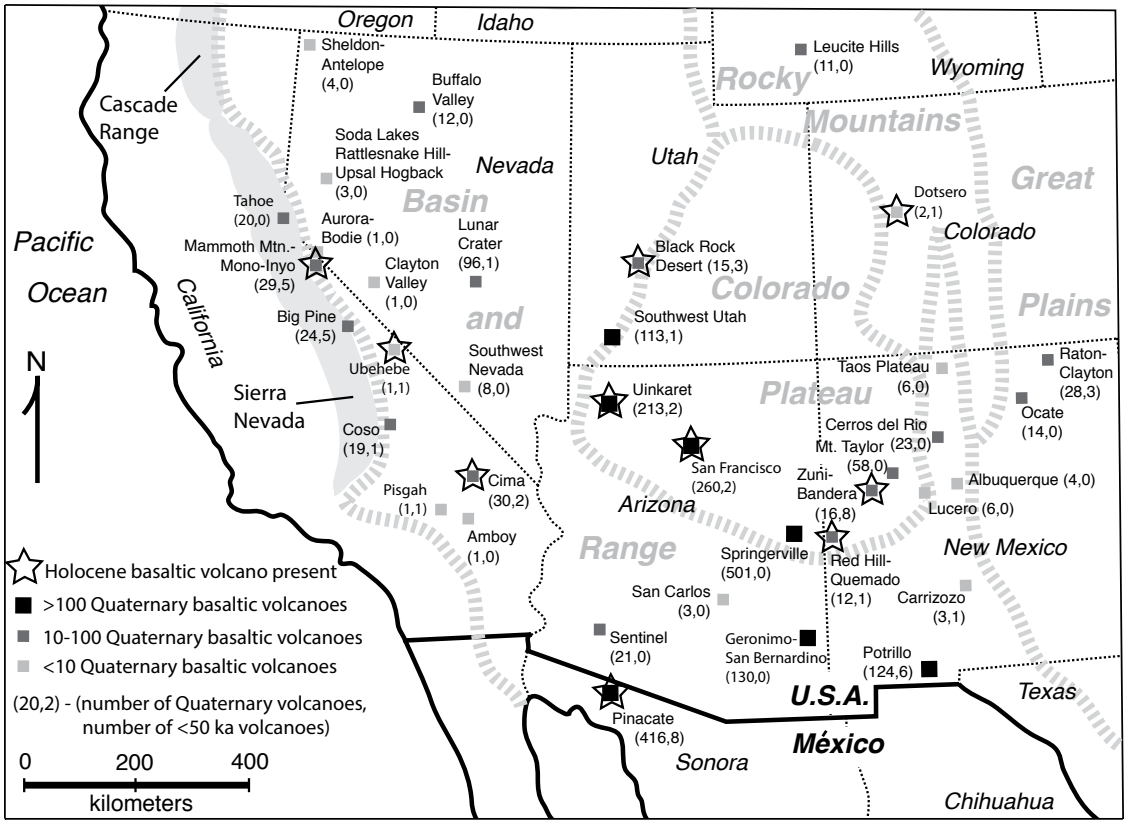

Figure 1. Distribution of basaltic volcanic fields in the American Southwest is shown with our best estimates of the number of Quaternary volcanoes as well as those with ages of <50 ka in each field. Fields with dated Holocene volcanoes are also indicated. Geologic provinces are shown, including, from east to west: Great Plains, Rocky Mountains, Colorado Plateau, and Basin and Range. The Sierra Nevada and southern part of the Cascade Range, both parts of the Pacific Province, are also indicated.

during their eruptive episodes (e.g., fractionation and assimilation and arrival of different magma batches, as at Parícutin, México, or Mount Gambier, Australia; Erlund et al., 2010; van Otterloo et al., 2014) while also tapping different primitive melts from the mantle source region (e.g., McGee et al., 2012). Some workers use the term *polymagmatic* to indicate these complexities within the context of a monogenetic volcano (see McGee and Smith, 2016).

Monogenetic volcanoes tend to form volcanic fields, i.e., definable areas within which volcanoes are scattered. Volcanic fields typically have lifespans on the order of a few million years and can contain hundreds of individual volcanoes down to a single volcano (Valentine and Connor, 2015). The spatial distribution of volcanoes within such a field can be completely random, but more often volcanoes form alignments and clusters. Clusters can involve many overlapping volcanoes; they suggest either a focused source of magma genesis in the upper mantle, a crustal mechanism that facilitates magmas reaching the surface within the cluster compared to the surrounding areas, or some combination of the two (Tadini et al., 2014). Individual clusters can have high spatial densities of volcanoes that overlap, and they can have lifespans of a million years or more (e.g., Conway et al., 1997).

Around 1990, the term *polycyclic* was suggested for scoria-cone volcanoes that show evidence of having had long time gaps (thousands to tens of thousands of years or more) between eruptions (see Wells et al., 1990). Wells et al.'s (1990) case study, Lathrop Wells volcano in Nevada, was later shown definitively to have had a single eruptive episode (Heizler et al., 1999; Valentine et al., 2007). The term polycyclic is itself polycyclic, as it has recently been reappearing in the literature (e.g., Wenger et al., 2017; Poblete Piedrabuena et al., 2019), often based upon paleosols interbedded with tephra units and/or varying degrees of geomorphic degradation at a volcanic center. We note that in any volcanic field, there is a finite probability that a new volcano will overlap, or even be fully co-located with, a previously formed volcano, and this is especially true in clusters. Such overlapping or co-located volcanoes, which

can have paleosols and unconformities between their deposits and different degrees of degradation, nevertheless are normally monogenetic in that they do not show evidence of being related via a single long-lived, crustal magma reservoir. Although this is mainly just a semantics issue, we avoid the term polycyclic because, whether intentional or not, it can imply long-lived magma reservoirs in the same sense as one associated with a polygenetic volcano.

The basaltic volcanoes discussed here can record a range of eruptive styles that include relatively quiet effusion of lava to explosive styles. For explosive activity, we use the terms *Strombolian* and *Hawaiian* in a strict sense to indicate eruptive styles dominated by individual bursts of coarse juvenile lapilli and bombs (*Strombolian*) and sustained discharge of similarly coarse, fluid juvenile clasts (*Hawaiian*). *Violent Strombolian* refers to sustained or rapidly pulsing eruption of a mixture with sufficient fine lapilli to ash that a convective tephra plume results and attendant fallout deposits are distributed over distances of kilometers to tens of kilometers (originally described during the 1943–1952 C.E. eruption of Parícutin, México; see Luhr and Simkin, 1993). Valentine and Gregg (2008) discussed the requirements for a sustained or rapidly pulsing eruption to have violent Strombolian behavior versus Hawaiian and recognized a spectrum of behaviors in between. They also defined violent Strombolian activity as producing eruption columns up to 10 km in height, with *sub-Plinian* activity ranging from 10 km to 20 km high. Strombolian, Hawaiian, violent Strombolian, and sub-Plinian eruptions are driven primarily by exsolution and expansion of magmatic volatiles. Monogenetic eruptions dominated by phreatomagmatic explosive activity can produce *maar-diatremes* (White and Ross, 2011), which have craters that cut into the pre-eruptive landscape and are surrounded by low-profile tephra rings. *Tephra rings* include deposits of fallout, pyroclastic currents (pyroclastic surges, dominantly), and ballistic clasts and normally contain abundant lithic clasts that can be dominant relative to juvenile clasts. *Tuff rings* and *tuff cones* have crater floors at or above the pre-eruptive ground level, and low- to high-angle slopes, respectively; they are commonly associated with shallow groundwater- or surface water-magma explosions. Juvenile material in such features is often highly altered to palagonite.

Approach

Much of this paper is a literature review, including a compilation of the number of Quaternary basaltic volcanoes and age determinations in the region (Table S1 [see footnote 1]). The objective in this compilation was to assess the completeness and gaps in geochronologic data on the scale of the entire American Southwest and to provide a basis for our simple regional recurrence rate calculations. The data originate from journal papers as well as state and national geological survey reports and graduate theses. In general, we reported any readily accessible, published date for which sample locality could be identified, and we did not filter these by which were thought to be most accurate. In many examples, multiple determinations were published for individual volcanoes, and where the data from those are given in the source publication, and unless otherwise noted, we report all of them rather than the weighted mean. Often both plateau and isochron ages are presented in original sources for $^{40}Ar/^{39}Ar$ age determinations; in such cases, we report the preferred age if that is stated by the original author or the plateau age if a preference is not given. Many volcanoes were dated by older K-Ar methods, and these ages are reported here if their source document is readily accessible, although that method is typically not as reliable as the $^{40}Ar/^{39}Ar$ method for young basalts. The low potassium content of the basalts and low radiogenic yield make the K-Ar method very sensitive to the composition of initial trapped Ar and to analytical procedures and corrections (see summary by Heizler et al., 1999), and often result in the production of dates with errors of the same magnitude as the age itself. Other dates reported here include U-series, surface exposure ages (^{36}Cl, ^{10}Be, ^{3}He), ^{14}C, optically stimulated luminescence, and magnetic secular variation. Because much of the Southwest is arid, suitable material for ^{14}C dates is scarce, so this common dating technique is rarely used. Only ages that include some analytical information and error estimates are included in the compilation (with rare exception), which excludes relative geomorphic ages, for example. We stress the importance of readers studying the original sources before using the data in future analyses.

We estimate the recurrence rate (new basaltic monogenetic volcanoes per year) based upon the compiled dates and upon the total volcano count over the Quaternary Period. The former is incomplete because only a fraction of volcanoes has been dated, while the latter provides an upper bound (but with uncertainty due to potential errors in the volcano count), assuming a constant Quaternary rate and using a simple Poisson model. An important conclusion of our work is that more detailed mapping, physical volcanology, and geochronology are needed to reduce uncertainties and to provide insights into non-homogeneous processes such as spatial and temporal clustering of volcano occurrences both at the regional scale and at the scale of individual volcanic fields.

TABLE 2. SUMMARY OF QUATERNARY AND <50 KA BASALTIC VOLCANOES BY STATE[1]

State	Number of Quaternary basaltic volcanic fields	Number of Quaternary basaltic volcanoes	Number of <50 ka basaltic volcanoes
Arizona	6	1128	4
California	8	124	15
Colorado	1	2	1
Nevada	7	125	1
New Mexico	11	295	19
Utah	2	128	4
Wyoming	1	11	0
Sonora (México)[2]	1	416	8
Total	37	2229	52

[1]See Table S1 (text footnote 1) for data by volcanic field and data sources.
[2]Pinacate volcanic field is counted here because of its proximity to the USA-Mexico border.

REGIONAL AMERICAN SOUTHWEST TECTONIC SETTING

While we refer to Quaternary basaltic volcanism in the Southwest as *intraplate*, in detail it occurs in four different physiographic provinces that correspond to different tectonic-structural settings. The volcanism is most abundant in or near the Basin and Range Province and onto the bordering margins of the Colorado Plateau and Cascade-Sierra Nevada Ranges (Fig. 1). Two Quaternary fields extend into the Great Plains in northeastern New Mexico, and two additional fields are found in the Rocky Mountains Province.

Factors such as style of regional deformation, or absence of it, and crustal and lithospheric thicknesses play important roles in both magma origins and ascent to the surface. The Basin and Range Province is dominated by extensional tectonics and associated lithospheric thinning and normal faulting. The degree of thinning is related to the thickness of the pre-extension lithosphere and to the timing of the onset of extension at a given location. Broadly, Basin and Range has three parts. North of our region of interest, extension began as early as 45 Ma (Sonder and Jones, 1999) and gradually expanded to the south-southwest into our study area across northern and central Nevada and western Utah between 40 Ma and 25 Ma; this region forms the northern Basin and Range. The southern Basin and Range (southwestern and central New Mexico including the Rio Grande rift, southern Arizona, and southeastern California) has been extending since ca. 25 Ma (Sonder and Jones, 1999). Crustal thicknesses in the northern and southern part of the province are typically between 28 km and 35 km, while the lithosphere is ~70–80 km thick (Gilbert, 2012; Shen et al., 2013; Kumar et al., 2012). The central Basin and Range, a ~300-km-wide band that stretches from the western edge of the Colorado Plateau across southern Nevada, began extending around 16 Ma; the later onset of extension corresponds to still-thick crust and lithosphere up to ~45 km and ~125 km thick, respectively (Gilbert, 2012; Schulte-Pelkum et al., 2011). Deformation associated with the transform boundary between the North America and Pacific plates extends inland to the Walker Lane dextral shear zone (roughly coincident with the California-Nevada border) and is superimposed on the east-west extension in the western part of the Basin and Range Province (Putirka and Busby, 2011). Low levels of deformation due to relative plate motion also extend deeper into the Basin and Range (Hammond et al., 2014; Singleton et al., 2019).

The Colorado Plateau, compared to neighboring provinces, is a stable domain with minor tectonic deformation. It, along with the Rocky Mountains and Great Plains Provinces, has crustal thicknesses ranging mostly between 40 km and 50 km (Gilbert, 2012; Shen et al., 2013) and lithosphere-asthenosphere boundary depths of 90–135 km (Levander et al., 2011; Kumar et al., 2012). The provinces, with their differing regional tectonics, correspond to various levels of heat flow, with the northern and southern Basin and Range and the Rocky Mountains in our study area having local values above 105 mW/m^2, while heat flow at the Colorado Plateau and Great Plains is less than 62 mW/m^2 (Parsons, 2006).

Crustal basement and lithospheric mantle rocks beneath most of the Southwest are composed of Proterozoic terrains accreted to the margin of Laurentia (Baldridge, 2004). The Leucite Hills volcanic field in southern Wyoming (Fig. 1) erupted through older Archean basement, while Quaternary magmas in the northwestern part of the study region erupted through much younger, Mesozoic crust. These different lithospheric/crustal domains contribute to the geochemical signatures of basaltic rocks and aid in interpreting the roles of lithospheric versus asthenospheric partial melting in generating the magmas (e.g., Perry et al., 1988; Farmer et al., 1989, 2020; Crow et al., 2011).

OVERVIEW OF SOUTHWESTERN BASALTIC VOLCANOES

Volcano Count and Geochronology

In total, we identified 2229 basaltic volcanoes of Quaternary age (1813 in the USA; Tables 2 and S1 [footnote 1]; Fig. 1) in the Southwest. This count includes all basaltic volcanoes that are mapped as Quaternary whether they have a quantitative age determination or not. The count primarily consists of vent structures shown on published geologic maps, in some cases augmented by satellite imagery, and does not account for co-eruptive vents; this simplification was necessary because little or no physical volcanological work, which would identify co-eruptive vents, has been conducted on the vast majority of the volcanoes. It does not account for an unknown number of (mostly) older, buried Quaternary volcanic centers; burial can result from emplacement of younger volcanic products as well as from alluvial sediments in subsiding basins (e.g., Valentine and Perry, 2009). Some of the volcano counts (for example, the Geronimo-San Bernardino and San Francisco fields) are estimates from the literature rather than actual counts that we conducted due to the buried-vent uncertainty in these very active fields. Table S1 provides details of volcano counts and a full list of the 789 readily accessible age dates that we compiled and their references. Of the 2229 Quaternary volcanoes we tabulated, ~548 have been dated. In many cases, multiple determinations have been completed for individual volcanoes, and these are indicated in Table S1, but in some cases (namely the Cima volcanic field), the published information makes it difficult to positively identify to which volcano a given age date corresponds; this means that the 548 may be an overcount by around 20–30 volcanoes, but further quantification would require new fieldwork to determine how the published ages match to specific centers. Of particular interest from a shorter-term hazard perspective, 52 volcanoes are dated to less than 50 ka (Fig. 1); this count only includes volcanoes for which a quantitative age determination is available to assure their young age, and for cases with multiple age determinations, it is based on the median age.

Some of the volcanic fields produced basalts of Holocene age (see Table S1 [footnote 1] for dates and literature sources for the volcanoes listed below; Fig. 1). These include, in Arizona, Sunset Crater and Little Springs (San Francisco and Uinkaret fields, respectively). Holocene eruptions in California include A-Cone in the Cima field; Red Cones in the Mammoth Mountain-Inyo-Mono field; and at Ubehebe in Death Valley. Holocene volcanism in New Mexico produced two lavas in the Potrillo field, as well as tephra at Zuni Salt

Lake maar, and possibly at Cerro Pomo, in the Red Hill-Quemado field. The Zuni-Bandera field (New Mexico) has produced at least two Holocene flows (McCartys and Bandera). Dotsero is an isolated Holocene maar volcano in Colorado. In Utah, the Holocene Ice Springs volcano is found in the Black Rock Desert field. Finally, in the Pinacate field in Sonora (Mexico), La Laja cone is of Holocene age, and others are just older.

Petrogenesis and Ascent

Southwestern basaltic magmas range from tephrites to basaltic trachyandesites (e.g., Fig. 2) and record varying degrees of partial melting (generally less than ~5%; e.g., Cortés et al., 2015) in both lithospheric and asthenospheric mantle sources (e.g., Farmer et al., 1989; Reid et al., 2012). Although we focus only on basaltic volcanoes, some of the fields we tabulated include more evolved eruptive products. We return to this briefly in our Discussion. Geochemical data for the fields are scattered in many publications, databases, and theses and are not comprehensive for most of the volcanic fields. The five major volcanic fields shown in Fig. 2A, each having ~100 or more Quaternary volcanoes, are described in more detail in Section 5; they have the most comprehensive data sets and show that there are considerable differences in compositional trends for different fields.

Mantle source compositions for the mafic volcanoes are heterogeneous on a range of scales, from ~500 m, based upon data from closely spaced volcanoes (Rasoazanamparany et al., 2015), to regional scales with contrasting lithospheric and asthenospheric sources (e.g., Reid et al., 2012; Cousens et al., 2013). The heterogeneities result, at least in part, from fluids emplaced in the upper mantle (metasomatism) during the long early Proterozoic to early Paleogene history of subduction events off what is now the west coast of North America, as well as longer-term recycling of oceanic crust within the mantle (e.g., Reid et al., 2012; Rasoazanamparany et al., 2015; Farmer et al., 2020). A range of geodynamic models has been explored as explanations for basaltic volcanism in the Southwest and, in particular, its concentration along the margins of the Colorado Plateau and Sierra Nevada (Table 3). These models involve processes such as edge convection and/or delamination, where the lithospheric thickness changes over a short distance, shear-driven upwelling, and slow heating of lithospheric mantle that is eventually replaced by asthenospheric mantle during lithospheric thinning (e.g., Perry et al., 1988; van Wijk et al., 2010; Reid et al., 2012; Ballmer et al., 2015). In areas where magma sources are within thick lithospheric mantle, such as the central Basin and Range, compositional variability due to metasomatic processes likely results in local small domains of partial melt under static ambient conditions even with no active decompression such as during upwelling; these small domains may feed the sparse volcanoes at the surface there (Valentine and Perry, 2007). Melting depths across the Southwest have been estimated at ~30–130 km and temperatures at ~1200–1650 °C (e.g., Gazel et al., 2012; Cortés et al., 2015; Plank and Forsyth, 2016).

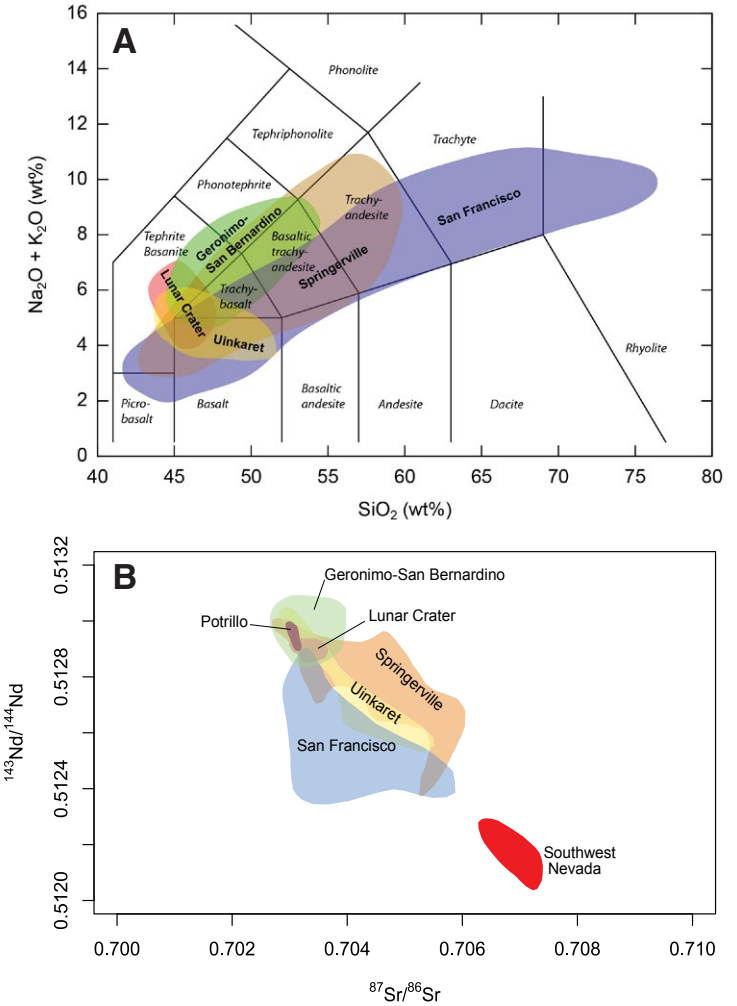

Figure 2. (A) Diagram shows total alkali-silica for five major volcanic fields (~100 or more Quaternary volcanoes), namely Springerville, Geronimo-San Bernardino, San Francisco, Uinkaret, and Lunar Crater. Data fields are from Mnich and Condit (2018), Kempton et al. (1987), Arculus and Gust (1995), Crow et al. (2015), and Cortés et al. (2015). (B) Nd-Sr isotope ratio plot for six major volcanic fields; data are from Rudzitis et al. (2016), Crow et al. (2011), Kempton et al. (1990), Kempton et al. (1987), Condit et al. (1989), Rasoazanamparany et al. (2015), Thompson et al. (2005), and unpublished data are from Michael Ort. Included for comparison is the Southwest Nevada volcanic field, which is one of the smallest fields and is interpreted to be sourced from lithospheric mantle with little or no crustal contamination during ascent (Valentine and Perry, 2007).

TABLE 3. MODELS FOR BASALTIC MAGMA GENESIS IN THE SOUTHWEST

Conceptual model	Applicable area	References
Upwelling asthenosphere with heating (thermal conversion) of sub-continental lithosphere and eventual replacement by asthenosphere.	Basin and Range (including Rio Grande Rift).	Perry et al. (1988); Roy et al. (2009)
Edge convection at step in lithosphere thickness, including upwelling asthenosphere and downwelling lithosphere (delamination or drips) with attendant heating of lithospheric mantle.	Margins of Colorado Plateau and eastern front of Sierra Nevada. Northern Basin and Range.	Roy et al. (2009); van Wijk et al. (2010); Levander et al. (2011); Reid et al. (2012); Cousens et al. (2013); Rudzitis et al. (2016)
Upwelling of asthenosphere near lithospheric keel due to relative motion of lithosphere and asthenosphere.	Margins of Colorado Plateau and transition from Mesozoic to Proterozoic lithosphere (west to east) in northern Basin and Range.	Ballmer et al. (2015); Roy et al. (2016)
Shear-driven upwelling.	Margins of Colorado Plateau, eastern front of Sierra Nevada, Basin and Range.	Conrad et al. (2010); Gazel et al. (2012); Ballmer et al. (2015)
Deformation-driven focusing of melt in heterogeneous lithospheric mantle.	Central Basin and Range.	Valentine and Perry (2007)

Some basaltic magmas may have ascended quickly from source depths, whereas others stalled at the crust-mantle interface and/or within the crust (e.g., Valentine and Perry, 2007; Cortés et al., 2015). Exposures of pre-Quaternary, deeply eroded analogs to the younger volcanoes indicate that magma ascent was primarily via dikes; sills, where protracted fractionation processes could occur, formed at a range of depths including as shallow as ~200 m (Delaney and Gartner, 1997; Valentine and Krogh, 2006; Re et al., 2015; Richardson et al., 2015; Muirhead et al., 2016; Germa et al., 2020). Changes in the shallow dike and sill systems during eruptions can play an important role in the resulting eruption processes (Genareau et al., 2010).

Landforms and Deposits

Landforms and deposits, which reflect eruption mechanisms and magma properties, run the full gamut that can be expected at subaerial (or shallow subaqueous) basaltic volcanoes. The most abundant landforms are scoria cones and ramparts and associated lava flows. Scoria cones and ramparts are dominated by coarse lapilli and bombs with varying degrees of welding (agglomerates). The few volcanoes that have been studied in detail commonly have associated tephra deposits that can extend kilometers to tens of kilometers from source vents and record magmatic volatile-driven explosive activity that includes Strombolian, Hawaiian, violent Strombolian, and sub-Plinian in intensity and style (Valentine et al., 2007; Ort et al., 2008a, 2008b; Browne et al., 2010; Johnson et al., 2014; Alfano et al., 2019; Zawacki et al., 2019). Lava flow fields include ʻaʻā and block lavas to pāhoehoe and reflect a wide range of effusion rates and flow dynamics (Figs. 3A–3B; Zimbelman and Johnston, 2001; Soldati et al., 2017; De Hon and Earl, 2018; Hamilton et al., 2020). Many lava fields contain abundant rafts of pyroclastic material that originated by slumping of portions of the source cone or rampart onto exiting lavas, which demonstrates complex relations between cone building by explosive activity and destruction by slope failure and transport atop lavas (e.g., Holm, 1987; Riggs and Duffield, 2008; Valentine et al., 2006; Younger et al., 2019).

The degree of surface degradation of lava fields and cones/ramparts is taken as a relative age indicator in the field by many workers (Figs. 3A–3B; e.g., Wood, 1980; Wells et al., 1985; Hooper and Sheridan, 1998). Very fresh lava surfaces that preserve in detail their original emplacement features may be mapped as Holocene, while more degraded surfaces with soils on top, which can also show the earliest stages of inverted topography, are mapped as Pleistocene. Similarly, cones and ramparts that show no sign of erosion are sometimes mapped as Holocene, while those showing initial rill erosion of outer slopes to erosional exposure of ventward-dipping pyroclastic beds are normally mapped as late Pleistocene. When erosion of the surrounding landscape has produced inverted topography (valley-filling lavas converted to mesa-capping units) and feeder dikes and necks are exposed, a volcano may be mapped as pre-Quaternary. In detail, these relative age methods, which are largely informal, can be complicated by many factors in the semi-arid to arid Southwest, including: (1) original volcanic facies such as welded or nonwelded cone deposits; (2) how much of a lava surface is initially covered with tephra or rafted pyroclastic deposits; (3) pre-eruptive topography and competence of rocks that surround and/or underlie a volcano; (4) local climate and vegetation; and (5) local flux of eolian sediment onto volcanic surfaces (Wells et al., 1985; Valentine et al., 2006, 2007). The complicating factors make one-to-one comparison of the morphology of different volcanoes difficult. Despite these issues, the qualitative, informal field judgements described above are often the basis for units being mapped as Quaternary versus Tertiary on geologic maps and are reflected in our volcano counts (Table S1).

Phreatomagmatic landforms occur in most of the Southwestern fields and typically form ~10% or less of the volcano types. Among these, maars (maar-diatremes) are the most common; they record highly explosive interaction of magma and groundwater (Fig. 3D; White and Ross, 2011; Valentine and White, 2012). Many maar volcanoes switched between magmatic volatile-driven and phreatomagmatic eruption processes during their lifetimes and produced

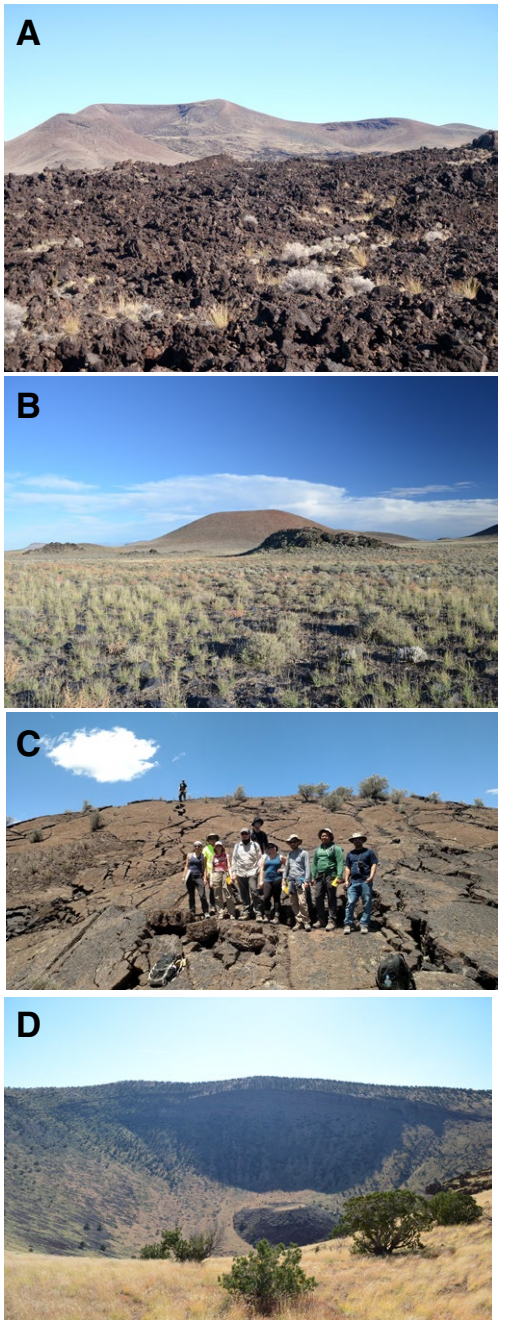

Figure 3. Examples of volcano morphology from around the Southwest are shown. (A) View across the top of 'a'ā lava field toward its source, which is the high cone in the background on the left side (Marcath volcano, ca. 35 ka, Lunar Crater volcanic field; Younger et al., 2019). The cone summit is ~280 m higher in elevation than the lava surface shown. (B) View across an older (190 ka), but originally similar, lava field in Lunar Crater volcanic field shows smoothing of the lava surface over time. Source cone (background) is ~100 m tall. (C) Smooth surface of an inflated lava field (McCarty's flow, ca. 3.5 ka, New Mexico). (D) View across Colton Crater, a maar-diatreme volcano in the San Francisco volcanic field (Arizona). Crater diameter is ~1.2 km and depth (from high part of rim) is ~300 m. Note late-stage scoria cone on crater bottom.

complexes of craters (e.g., Ubehebe volcano, California; Fierstein and Hildreth, 2017) and overlapping cones, craters, and ramparts (Valentine and Cortés, 2013; Amin and Valentine, 2017; Sweeney et al., 2018) during single monogenetic episodes. Tephra rings record emplacement of pyroclastic deposits via ballistic, fallout, and pyroclastic current mechanisms. Some of the original studies that identified the genetic relation between dune-bedded deposits and pyroclastic surges (a.k.a. base surges or dilute pyroclastic currents) were conducted at Quaternary Southwestern maar volcanoes (Fisher and Waters, 1970; Crowe and Fisher, 1973). Tuff cones, which normally form during eruption through shallow water, are associated with some basins that contained lakes during the Pleistocene epoch (e.g., Pahvant Butte, Utah; White, 2001).

MAJOR VOLCANIC FIELDS

Below we provide overviews of volcanic fields with ~100 or more Quaternary basaltic volcanoes (Table 4). These include: Potrillo (New Mexico); Springerville, San Bernardino-Geronimo, San Francisco, and Uinkaret (Arizona); Southwest Utah; Lunar Crater field (Nevada); and the Pinacate volcanic field (Sonora, Mexico). Two maps are provided for each field: (1) an unlabeled shaded relief map that is intended to help the reader visualize the terrain and volcanic morphology and (2) satellite images showing most vent locations with major features that include regional faults and with place names labeled. More detailed geologic maps can be found in the references cited for each field. The scales and areas covered by the two maps of a given field are identical. Volcano ages reported in the text are provided with their source references in Table S1 (footnote 1).

Potrillo (New Mexico)

The Potrillo volcanic field of southern New Mexico (Fig. 4, Table 4) lies within the Rio Grande Rift portion of the Basin and Range Province. The field contains ~124 Quaternary vents, six of which have been dated to 50 ka or younger (Dunbar, 2005). Most of the landforms are scoria cones with extensive lava fields; very little physical volcanological research on eruptive products has been conducted in the Potrillo field. Aden Crater is a young flow with

TABLE 4. VOLCANO COUNTS AND DATES FOR MAJOR VOLCANIC FIELDS

Volcanic field (state)	Approximate area (km^2)*	Age range (Ma)	Number of Quaternary volcanoes	Number of published dates	Main compositions
Potrillo (New Mexico)	3000	Not constrained	124	22	Basanite, trachybasalt, basalt
Springerville (Arizona)	5500	0.3–2.1	501	37	Basalt (tholeiite), trachybasalt, basaltic trachyandesite
Geronimo-San Bernardino (Arizona)	1000	0.26–9.2	130	5	Basanite, trachybasalt, basaltic trachyandesite
San Francisco (Arizona)	9000	0.001–6	260	83	Basalt, trachybasalt to trachyte, rhyolite
Uinkaret (Arizona)	3000	0.001– 3.6	213	37	Basalt, trachybasalt
Southwest Utah (Utah)	12000	0.027–5.3	113	107	Basalt, basaltic andesite, trachybasalt, basaltic trachyandesite
Lunar Crater (Nevada)	500	0.035–5.94	96	17	Basanite, basalt, trachybasalt
Pinacate (Sonora, Mexico)	3500	0.011–1.7	416	29	Basanite, basalt, trachybasalt, basaltic trachyandesite

Note: See text and Table S1 (text footnote 1) for details including references.
*Area is for part of volcanic field active during Quaternary Period and does not include older parts.

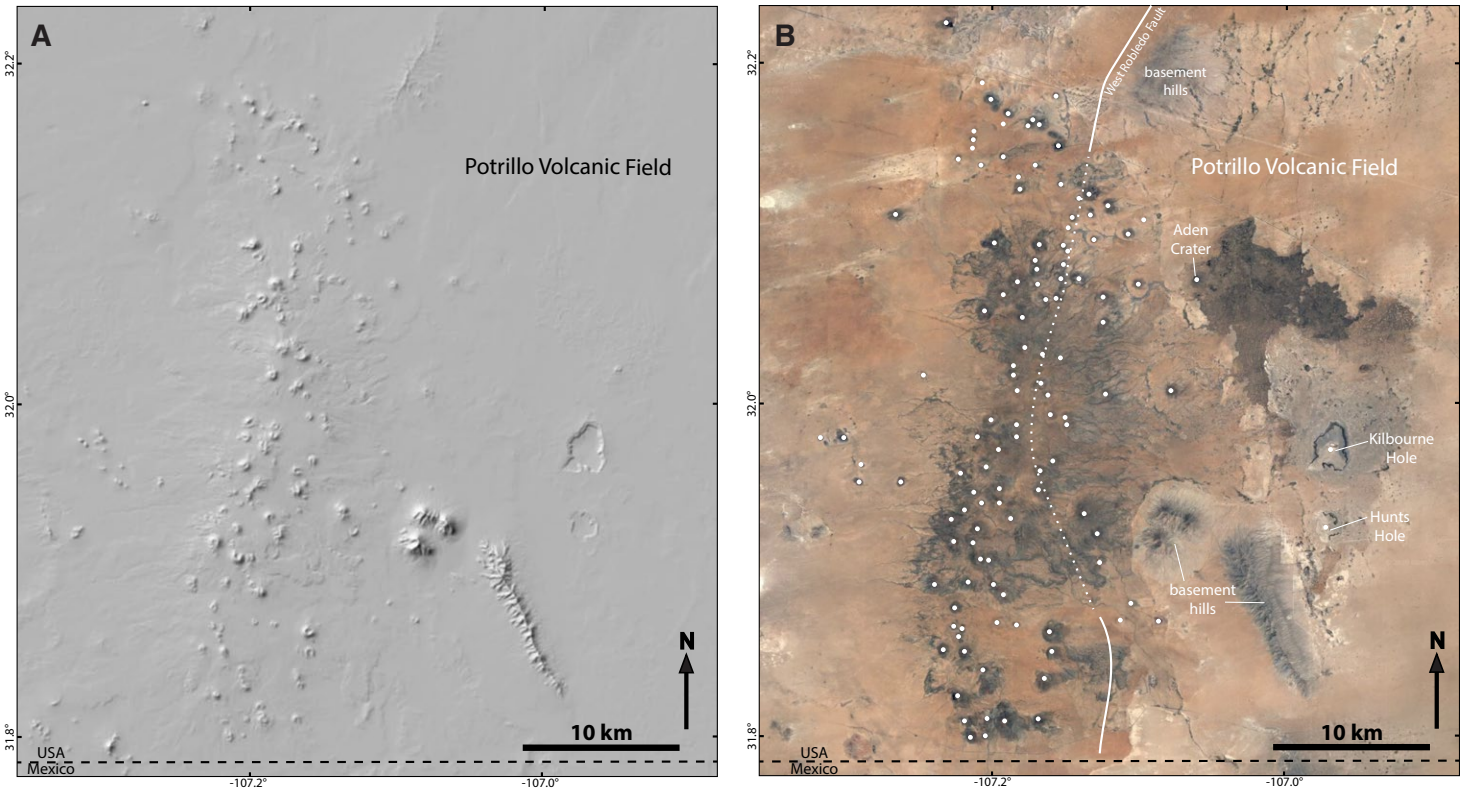

Figure 4. (A) Shaded relief map shows the Potrillo volcanic field, southern New Mexico (from U.S. Geological Survey site https://apps.nationalmap.gov/3depdem; accessed June 2021). (B) Google Earth image of the main part of the field. One additional center, Potrillo maar, lies just south of the area shown, and two isolated, small scoria cones lie ~20 km northeast of Kilbourne Hole; a few additional vents lie up to ~20 km north and south of the area shown, but it is not known if they are of Quaternary or older age. White dots mark vents identified in remote imagery, but detailed mapping would be necessary to determine if each vent records an individual monogenetic event (as opposed to some events producing multiple vents). "Basement hills" refers to pre-Quaternary rocks exposed at the surface; most of the landscape is dominated by eolian sands and alluvium. Thick line shows approximate trace of the West Robledo fault (down to the east) and is dotted where uncertain (Thompson et al., 2005).

well-preserved lava morphology (De Hon and Earl, 2018) and has a ^{3}He surface exposure age of ca. 22 ka (Table S1 [footnote 1]). Two young maars, Kilbourne Hole and Hunts Hole (ca. 24 ka and 16 ka, respectively) are well known for their ultramafic and crustal xenoliths (Bussod and Williams, 1991; Thompson et al., 2005; Cipar et al., 2020). Most vents lie within a north-northeast–trending band of ~10 km wide (Fig. 4) that roughly follows the inferred trace of the West Robledo fault, a Rio Grande Rift-related structure. The two maars mentioned above, plus Potrillo maar to the south of the area shown in Fig. 4, in Mexico, lie to the east of that concentrated band in an area of sparse vents.

Thompson et al. (2005) showed that lava compositions are basanites, trachybasalts (hawaiites), and basalts and determined that basaltic melts originated in young lithospheric mantle that "froze" recently (within the last ~20 m.y.) against the base of older, ~70-km-thick Proterozoic lithosphere. This younger lithospheric mantle was subsequently veined by hydrous melts derived from below, such that it locally contained amphiboles and then was reheated and partially melted by mantle upwelling beneath this part of the Rio Grande Rift. This most recent reheating produced the magmas, which in a small number of cases present geochemical evidence of amphibole-bearing source lherzolite that fed the Quaternary volcanism at Potrillo.

Springerville (Arizona)

The Springerville volcanic field in east-central Arizona has 501 identified vents that erupted between 2.1 Ma and 0.3 Ma, and lavas cover ~3000 km^{2} (Fig. 5, Table 4; Condit and Connor, 1996; Mnich and Condit, 2018). Condit and Connor (1996) summarize years of mapping efforts by several workers and show that eruptions occurred both in vent clusters and along fault-controlled alignments. These faults are parallel or perpendicular to the edge of the Colorado Plateau a few kilometers south of the field and are probably related to the extension of the Transition Zone, a region between the highly extended Basin and Range and stable Colorado Plateau. Condit et al. (1989) suggested the locus of volcanism shifted eastward at 1–3 cm/yr, which is consistent with motion of the North American plate over a stationary magma source (note that such plate motion-aligned progression is not common in the Southwest).

A complete dynamic digital map available online (Condit, 2010) presents dates, petrology, field relations, and many other important attributes of the field. Mnich and Condit (2018) explain the reasoning process for the mapping, one that builds upon that used in the San Francisco volcanic field by the U.S. Geological Survey (USGS) in the 1970s and that can be a model for the mapping of other volcanic fields. The volcanic field is broadly basaltic with no intermediate or silicic lavas. The 1.8 m.y. of eruptive activity is divided into three episodes (Condit and Connor, 1996; Mnich and Condit, 2018). From 2.1 Ma to 1.75 Ma, large volumes of tholeiitic lava erupted and made the basal flows of the field upon which the scoria-cone field was constructed. The magmas were derived from depths near the lithosphere-asthenosphere boundary (~100 km; Mnich, 2019). From 1.75 Ma to 1 Ma, alkali-olivine basalts erupted, which produced the bulk of the field's lava flows, especially in the east, with an increase in alkalic nature over time. From 1 Ma to 0.3 Ma, activity waned, and there were fewer and smaller eruptions. During these last two phases, magmas were sourced from smaller degrees of partial melting, relative to earlier volcanism in the field, as shallow as ~65 km (lithospheric mantle) to as deep as ~140 km, and trace element compositions indicate heterogeneous sources (Mnich, 2019). No eruptions are known to have occurred over the past 300,000 years.

Geronimo-San Bernardino (Arizona)

The Geronimo-San Bernardino volcanic field in the southeastern corner of Arizona, just north of the U.S.-Mexico border, consists of 130 Quaternary volcanoes (Table 4; Biggs et al., 1999) within the San Bernardino and San Simon Valleys and the Peloncillo, Perilla, Chiricahua, and Pedregosa Mountains on either side of them (Fig. 6). The valleys are separated by a subtle drainage divide and are part of the same graben structure with the mountain ranges on either side separated from the valleys by high-angle normal faults. The valleys extend for several hundred kilometers in Mexico and the United States, but the Pleistocene volcanism is located at the intersection of north-south–trending Basin-and-Range faults with northeast-southwest–trending older faults (Kempton and Dungan, 1989), which is mostly north of the international border. Some weak north-south vent alignments may trace buried graben-bounding faults. Limited isotopic dating (Kempton et al., 1987; Biggs et al., 1999) shows the Pleistocene volcanism is as young as ca. 260 ka, but this is poorly constrained. The volcanoes are all monogenetic, consisting of scoria cones interpreted as being from Strombolian activity and maars formed by explosive magma/groundwater interactions (Biggs et al., 1999). Lava flows were emitted from many vents, although not all lava flows have been linked to their vents.

Volcanism in the volcanic field is divided into two groups: Mio-Pliocene alkaline volcanism exposed in the mountains on either side of the valley (similar flows may be buried in the valley itself, but none crop out) and Quaternary (3.6–0.26 Ma) basanites and hawaiites that form the scoria cones, maars, and lava flows of the valley itself. Mafic, ultramafic, and granulitic xenoliths and megacrysts of aluminous augite, olivine, spinel, plagioclase, and anorthoclase are common in these younger rocks. Steep, rare-earth element (REE) curves with a limited range of heavy REEs are consistent with generation of the basalts from a garnet-bearing source. The basalts and ultramafic xenoliths have oceanic-island basalt (OIB)-like Sr and Nd isotopic signatures (Fig. 2B) with a time-integrated depletion in incompatible trace elements. Kempton and Dungan (1989) interpret this to indicate upwelling and decompression melting of the asthenosphere during Basin-and-Range extension. Intrusion of this OIB-like magma into the lithosphere and lower crust is recorded in the xenolith textures and chemistry, which indicates the existence of a complex of sills and dikes from the asthenosphere well into the crust. Rapidly ascending magmas derived from the asthenosphere sampled the lithospheric section and brought the xenoliths to the surface.

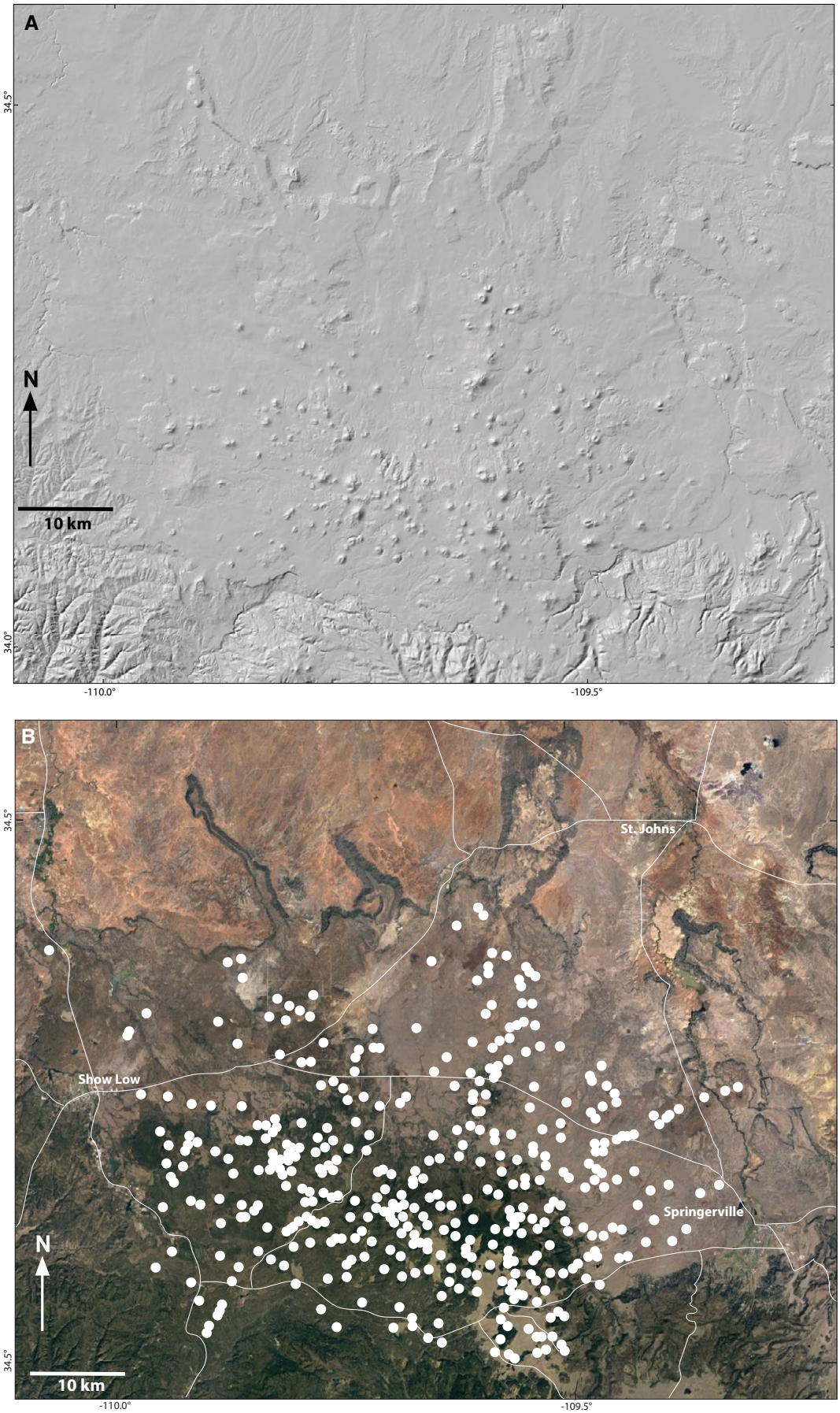

Figure 5. (A) Shaded relief map shows the Springerville volcanic field, eastern Arizona (from U.S. Geological Survey site https://apps.nationalmap.gov/3depdem). (B) Google Earth image of the field; white dots indicate basaltic vents (based on Condit and Connor, 1996).

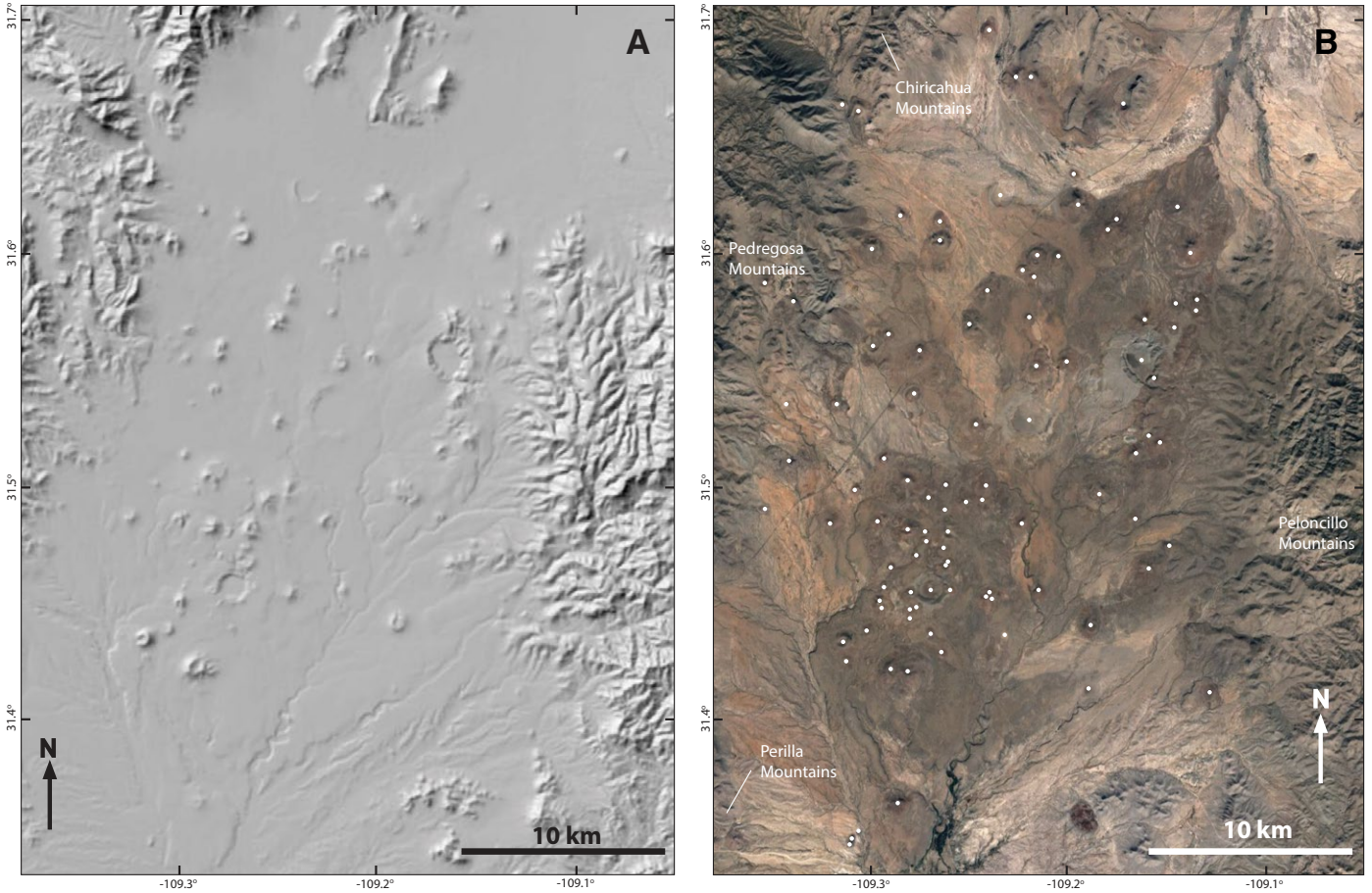

Figure 6. (A) Shaded relief map shows the Geronimo-San Bernardino volcanic field, southeastern Arizona (from U.S. Geological Survey site https://apps.nationalmap.gov /3depdem). (B) Google Earth image of the field; white dots indicate basaltic vents. The southern and eastern edges of the maps correspond with the borders between Arizona and Mexico and New Mexico, respectively.

San Francisco (Arizona)

The San Francisco volcanic field in north-central Arizona is one of the largest and most complex volcanic fields in the Southwest (Fig. 7, Table 4). Activity started around 6 Ma at the southwestern end of the field, near what is now Williams town, and has shifted generally east-northeastward since at a rate of 1.2–2.9 cm/yr, which is roughly equivalent to the North American plate movement (Tanaka et al., 1986). This direction of movement is also away from the Transition Zone, so the vent migration may correspond to the migration of extension. The field covers ~100 km west to east and 30–40 km north to south. Depth to the Moho increases from ~35–45 km over the field from southwest to northeast with recent activity through the greater crustal thickness (Reid et al., 2012). The volcanic field was mapped in the 1970s by a U.S. Geological Survey team that identified the vents for ~600 mafic monogenetic volcanoes (Wolfe et al., 1987a, 1987b; Moore and Wolfe, 1987; Newhall et al., 1987; Ulrich and Bailey, 1987; Holm, 1988).

Mafic volcanism has produced scoria cones, a few maars, and many lava flows. Many of the scoria cones are large (300 m in height), and many lava flows reach lengths of 8–12 km and thicknesses of many tens of meters. A few

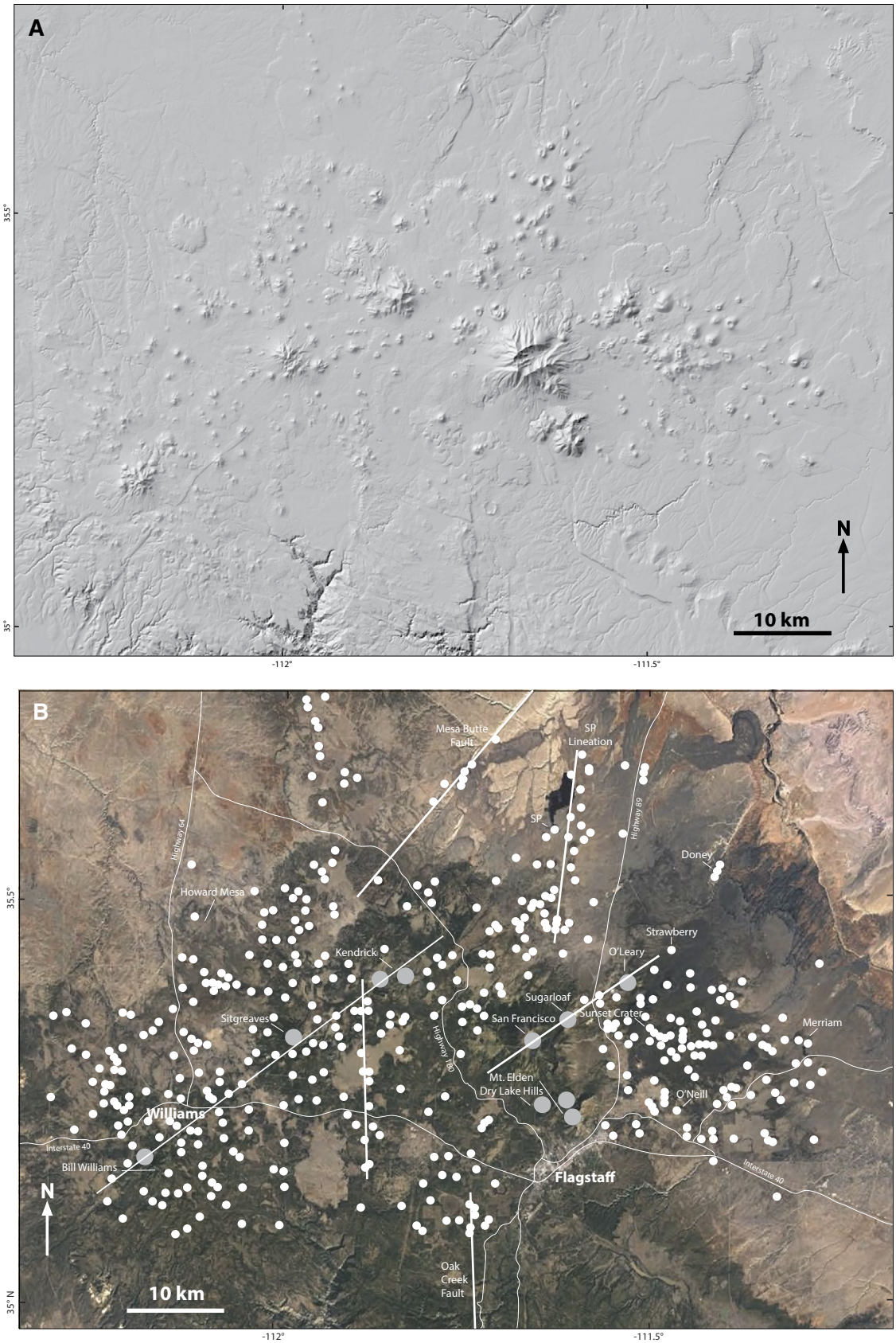

Figure 7. (A) Shaded relief map shows the San Francisco volcanic field, central Arizona (from U.S. Geological Survey site https://apps.nationalmap.gov/3depdem). (B) Google Earth image of the field; white dots indicate basaltic vents. The towns of Flagstaff and Williams are indicated along with major roads. Gray dots indicate intermediate to silicic volcanic centers. Thin lines are major roads and thick lines are faults and volcano alignments mentioned in the text.

eruptions brought lower crustal and cumulate xenoliths and mafic megacrysts up with the magmas, but these are not common. The San Francisco volcanic field shows trace element characteristics consistent with melting above the garnet stability field (Asmerom, 1999). Reid et al. (2012) argue that decompression melting produces initial melts below the lithosphere-asthenosphere boundary, but these magmas are interpreted to then mix with magmas sourced in the Proterozoic lithospheric mantle. Seismic imaging shows evidence of foundering of the lithospheric mantle into the underlying asthenosphere, and there is debate over whether it is occurring by delamination or drips (Levander et al., 2011). In either case, asthenosphere then wells up to replace the lost lithosphere with associated decompression melting. Lithospheric mantle may either be entrained into this upwelling material and melt with it or may melt as the lithosphere itself extends and thins (Reid et al., 2012; Rudzitis et al., 2016). The resulting magmas are alkalic to sub-alkaline basalts. Some follow a deep crustal fractionation process to evolve along a hawaiite-mugearite-benmoreite-trachyte line (Arculus and Gust, 1995), magmas of which erupt mostly as scoria cones. About a dozen of the eruptions of this high-Na series, plus a few true basalts, produced a final dacitic to rhyolitic dome in the crater of the scoria cone, which implies that some magmas stall in the middle crust and evolve and may be intersected by a later batch of magma. These bimodal scoria cones/domes are mostly but not exclusively along the trend of the active Oak Creek fault and a parallel lineation to the west (Fig. 7B).

Conway et al. (1997, 1998) detailed the controls on scoria-cone locations by fault systems in the north-south SP Crater alignment and northeast-southwest–trending Mesa Butte fault system. They show that the ascending dikes are caught and oriented by the fault systems, which makes those areas particularly likely to have eruptions than the surrounding area. Another common vent alignment is west-southwest, such as near Sunset Crater (Fig. 7B); this alignment roughly parallels the boundary of the Colorado Plateau and normal faults of the Transition Zone in this region.

A characteristic that distinguishes the San Francisco volcanic field, relative to the other major fields summarized here, is the large volume of intermediate to silicic magma that has erupted. Six large, evolved centers (Bill Williams, Sitgreaves, Kendrick, San Francisco, O'Leary, and Mt. Elden/Dry Lake Hills; Fig. 7B) and a handful of smaller evolved centers (e.g., Howard Mesa, Slate Mountain) represent roughly half to two-thirds of the total erupted volume from the field of an unknown number of individual eruptions. These centers are located along northeast-southwest–striking alignments that probably correspond to major buried Proterozoic faults. The magmas evolve through crystal fractionation in the lower crust accompanied by crustal anatexis with limited fractionation and assimilation in the upper crust (Arculus and Gust, 1995).

The San Francisco volcanic field has had six scoria cone eruptions and one rhyolitic dome eruption in the past 100,000 years (Fig. 7B). Sugarloaf Dome erupted at the mouth of the Inner Basin of San Francisco Mountain at 91 ± 2 ka (Morgan et al., 2004), which produced a large tephra ring and domes (Sheridan and Updike, 1975). The age and size of this eruption hint at the presence of a geothermal resource beneath this portion of the volcanic field (Morgan et al., 2004). SP Crater is a large scoria cone (~250 m above base) with an 8-km-long lava flow that erupted at ca. 70 ka. Doney Crater erupted at ca. 67 ka along a fissure that produced a string of small cones situated above the Doney fault, which becomes a monocline a few hundred meters to the north. A stubby lava flow was emitted from the base of a scoria cone and flowed toward the lowlands to the east. O'Neill Crater is a 50 ka scoria cone breached by emission of its lava flow with a small dacite dome that extruded at the end of the eruption into the crater. The basaltic andesite has magma-mixing textures and SiO_2 contents that range from 52% to 59%. Strawberry Crater, which erupted at ca. 50 ka, is similar to O'Neill Crater in that it is a scoria cone and lava flow with a small dacite dome in the mouth of the breached crater (Moore and Wolfe, 1987). The Strawberry lava flow is ~2 km long and much larger in volume than the O'Neill flow. Merriam Crater, dated by Duffield et al. (2006) using several methods at 19 ka, formed during a complex eruption in which two scoria cones and two spatter rings produced widespread basaltic tephra and several lava flows, at least one of which flowed 10 km to the Little Colorado River gorge, cascaded into it, and then continued 25 km down the drainage (Duffield et al., 2006). The lava flow blocked the river, which then backed up and flowed around the blockage and eventually formed Grand Falls, where it poured back into its original drainage. The most recent eruption in the San Francisco volcanic field is that of Sunset Crater, dated at 1084–85 CE (Elson et al., 2011). Sunset Crater is a 290-m-high scoria cone that produced 0.52 km^3 (dense rock equivalent) of basalt as a scoria cone, lava flows, and tephra (0.16 km^3, 0.12 km^3, and 0.24 km^3, respectively; Alfano et al., 2019). The eruption began with a 10-km-long discontinuous fissure and then localized to its western edge at Sunset Crater. The central vent activity initially produced Strombolian cone-building eruptions and emitted two lava flows; one ponded on the uphill side of the vent and the other flowed ~11 km down a pre-existing valley (Alfano et al., 2019). While still emitting the lava flows, the eruption increased in violence and produced three sub-Plinian eruption columns and tephra layers (0.22 km^3). The last portion of the lava flows was produced just after these paroxysmal eruptions, and minor Strombolian activity continued for perhaps months. The eruption ended with a phreatic blast at the summit crater. Elson et al. (2011) and Ort et al. (2008a, 2008b) use many techniques to argue that the eruption occurred between August of 1084 and March of 1085 CE with the month-level precision based upon the immature corn found in the lava spatter and the lack of springtime reworking of tephra within the sequence (reworking occurred afterward). Brumbaugh et al. (2014) interpret that a 6.5 hours-long earthquake swarm in 2009 recorded a basaltic intrusion at 14–27 km depth ~5 km west of Sunset Crater along a trend parallel to the nearby Mesa Butte fault.

Uinkaret (Arizona)

Most of the Uinkaret volcanic field was mapped by Billingsley et al. (2001), and dates are reported in several papers about the Grand Canyon and Uinkaret

Plateau lavas (Tables 4 and S1 [footnote 1]); Fenton et al., 2001, 2013; Karlstrom et al., 2007; Crow et al., 2015). The volcanic field is just north of the western Grand Canyon (Fig. 8) near the western edge of the southern Colorado Plateau. Lava flows both cascaded into the Grand Canyon and erupted from vents within the canyon itself. Lava flows dammed the river at least 17 times and flowed downstream for tens of kilometers (Crow et al., 2015). Breakout floods from these dams, which occurred repeatedly in the past, would be a hazard from any future eruption into the Grand Canyon (Fenton et al., 2001). The volcanic field has been active since ca. 3.6 Ma, and Billingsley et al. (2001) identified 213 Quaternary vents, two of which erupted in the past 50,000 years (Fenton et al., 2001).

The Uinkaret volcanic field primarily consists of scoria cones with associated lava flows. The Toroweap and Hurricane faults are large Quaternary faults with north-south trends that control much of the topography in the area and appear to affect the locations of vents. Many eruptions occurred along north-south fissure vents and formed aligned cones; these alignments parallel the local bedrock joint and fracture systems (Billingsley et al., 2001). Uinkaret magmas range from sub-alkaline basalts through alkalic basalts to basanites (Fig. 2A). Mantle-derived peridotite xenoliths surfaced with many eruptions. Crow et al. (2011) interpret the Nd and Sr isotopic ratios (Fig. 2B) of lavas to indicate that the source of the magmas, at ~80 km depth, is mid-oceanic-ridge basalt-like asthenosphere. They show that this asthenospheric signature has increased with time and is consistent with ascent of asthenosphere as lithosphere either thinned or delaminated. Proterozoic compositional boundaries correlate with these areas of asthenospheric upwelling, which may indicate weaknesses that extend through the entire lithosphere and aid lithospheric replacement and magma ascent.

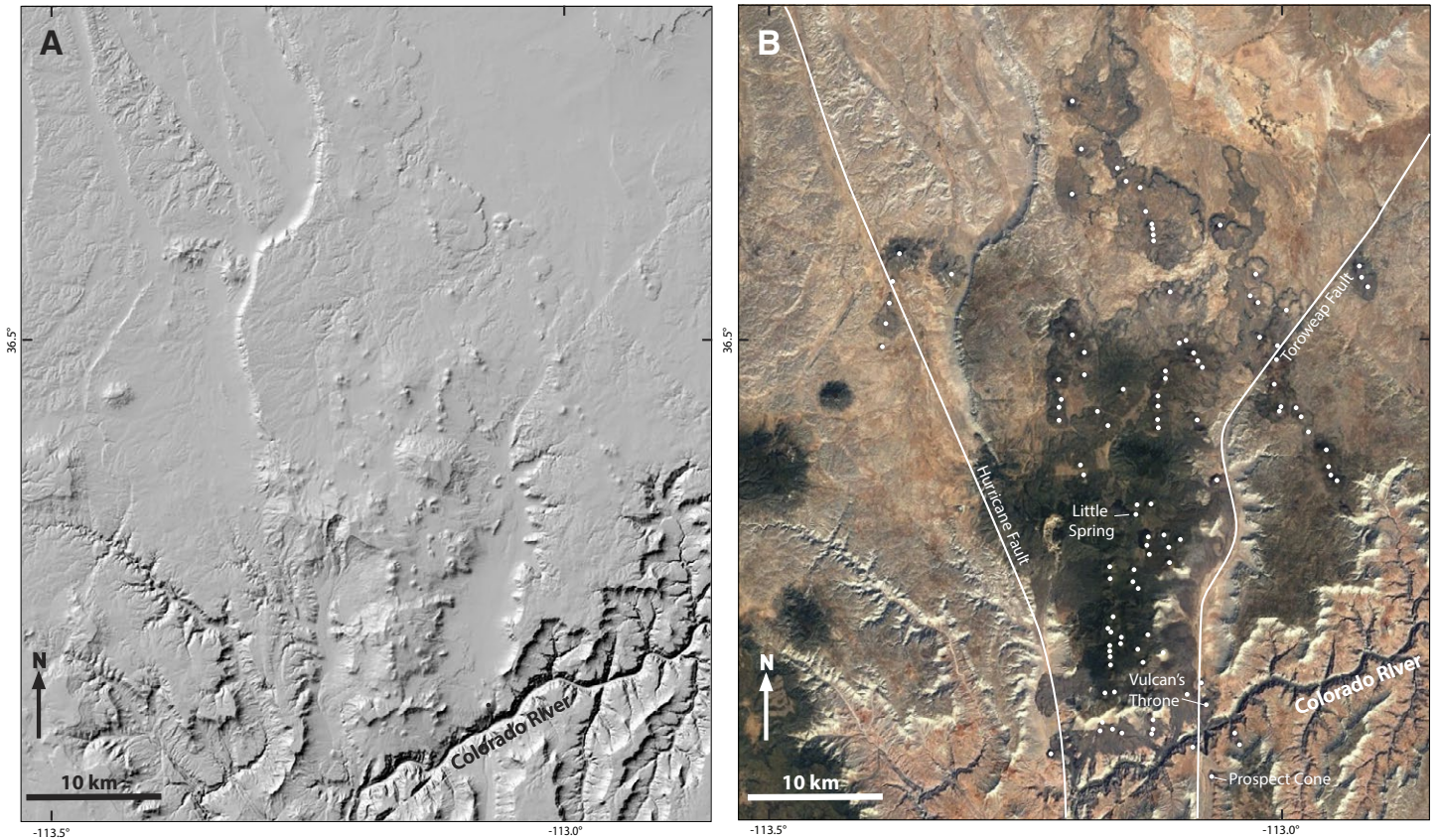

Figure 8. (A) Shaded relief map shows the Uinkaret volcanic field (from U.S. Geological Survey site https://apps.nationalmap.gov/3depdem). (B) Google Earth image of the area shows vents (white dots) and the Toroweap and Hurricane normal faults (both down to the west). The Colorado River runs at the bottom of the Grand Canyon.

The youngest eruptions of the field are the scoria cone and flows of Little Spring (1.3 ± 0.5 ka) and the basalt of Larrimore Tank (undated: Billingsley et al., 2001) on the Uinkaret Plateau and the basalts of Prospect Cone and Vulcan's Throne (37 ka and 73 ka, respectively) in the Grand Canyon. The Little Spring vent is a north-south–aligned spatter rampart at a topographic divide from which lava flowed both north and south. An area of spatter to the east of the main rampart contains very abundant dunite xenoliths and the Little Spring lava, and spatter is very rich in olivine crystals, many of which probably are from disaggregation of the xenoliths. Ceramic sherds dating to 1025–1200 CE have been found welded in Little Spring composite spatter clasts used in the walls of pithouses that date to about the same time period, which implies the eruption took place during that time period (Ort et al., 2008b). Native Americans also constructed trails and possible defensive battlements on the blocky surfaces of the lava flows and marked them with the same type of ceramic sherds as are found in the spatter. The lava flows in the Grand Canyon typically vented at the rim or along the sides of the canyon but then flowed down to the river channel. At the river, there is some evidence of lava-water interaction, but the lava generally overwhelmed the river and flowed a short way upstream and much longer distances downstream. The upstream lava is typically broken and shattered, perhaps from quenching, and thus eroded easily, but the downstream lavas tend to be more coherent and resistant to erosion and possibly endured as dams for millennia (Crow et al., 2015).

Southwest Utah

The Southwest Utah volcanic field covers a large area in Utah along the transition between the Basin and Range and Colorado Plateau provinces (Fig. 9, Table 4). Previous literature such as the Smithsonian volcano database (https://volcano.si.edu) and Wood and Kienle (1990) referred to subsets of the field under the names Kolob and Loa, Santa Clara, Bald Knoll, Markagunt Plateau, Hurricane, and Mineral Mountain-Cove Fort volcanic fields; we have integrated them into a single field because of their proximity to and relative continuity with each other. Hamblin et al. (1981) studied basaltic flows with an emphasis on their role in the geomorphic and uplift history of the region and took advantage of varying degrees of inverted topography of originally channel-confined lavas of different ages. Best et al. (1980) first characterized composition and age relations for basaltic rocks of Miocene through Quaternary ages. Smith et al. (1999) conducted a petrologic and geochemical study of a small portion of the field that is located along the Hurricane fault, which is the major bounding fault between the Colorado Plateau and Basin and Range Provinces in that area. They determined that the basanites and alkali basalts in this area resulted from a small percentage of partial melting of a heterogeneous lithospheric mantle source. Reid et al. (2012) included lavas from this volcanic field in their study of magma genesis along the entire southwestern margin of the Colorado Plateau and concluded that magma sources are mainly in lithospheric mantle that is being thermally reactivated due to thinning and upwelling associated with delamination along the transition to Basin and Range settings (see Table 3). Our compilation of ages was greatly aided by recent mapping, and associated reports including geochronology, by the Utah Geological Survey (Hintze et al., 2003; Rowley et al., 2005, 2006; Doelling 2008; Biek et al., 2010, 2011, 2015). Based upon these geologic maps, we count 113 Quaternary basaltic vent structures, one of which is dated at 50 ka or younger, but up to six others are potentially in that age range. The volcanoes all appear to be scoria cones with attendant lava flows; we did not find any maar craters on the maps. Although the maps and regional-scale geochemical studies cited above form a good framework, much of the Southwest Utah field is essentially unstudied from a physical volcanological and detailed petrologic/geochemical perspective.

Lunar Crater (Nevada)

The Lunar Crater volcanic field, like the San Bernardino-Geronimo, Potrillo, and Pinacate fields, lies well inside the extensional Basin and Range Province rather than near the province's margins. Although our count of mappable Quaternary vents totals 96 (Tables 4 and S1 [footnote1]), we include it here because it is likely that at least a few cones and flows are buried by younger products and within subsiding basins along the northwestern margin and the central portion of the field (Big Sand Springs Valley and Lunar Lake basin, respectively; Valentine et al., 2017); thus, it would meet our >100 vent criterion as a major volcanic field. Basaltic volcanism in the Lunar Crater field began at ca. 6 Ma in the southern part of the field, while the ~96 Quaternary vents occur only in its northern part (Fig. 10; note this rough age progression is oblique to North American plate motion). The ca. 35 ka Marcath Cone is the youngest volcano in the field (Shepard et al., 1995; Valentine et al., 2017).

The Lunar Crater field contains monogenetic volcano types ranging from scoria cones and fissure-fed agglomerate ramparts—both commonly accompanied by 'a'ā lava fields—to four maar craters. The Quaternary volcanoes are concentrated in a ~5-km-wide, 30-km-long, north-northeast–trending band (Fig. 10; note the pre-Quaternary portion of this field extends farther to the south-southwest; Valentine et al., 2017) that is roughly perpendicular to the orientation of the minimum principal compressive stress in the area. Within that band, clusters and alignments tend to share that orientation (Tadini et al., 2014). Several centers have been the subjects of physical volcanological studies. Younger et al. (2019) described the young Marcath lava field, estimating flow viscosities and documenting the role of rafted cone material in the lava morphology, while Johnson et al. (2014) documented the main tephra deposit associated with that eruption. Most activity in the Lunar Crater field was dominated by volatile-driven eruption styles such as Strombolian and Hawaiian (Valentine et al., 2017), but the maars record violent phreatomagmatic activity. Three of the maar craters formed during complex eruptions that began with Hawaiian fountaining and terminated with phreatomagmatic explosions (e.g., Easy Chair; Valentine and Cortés, 2013) or that switched back and forth between the explosive driving mechanisms (Bea's Crater; Amin and

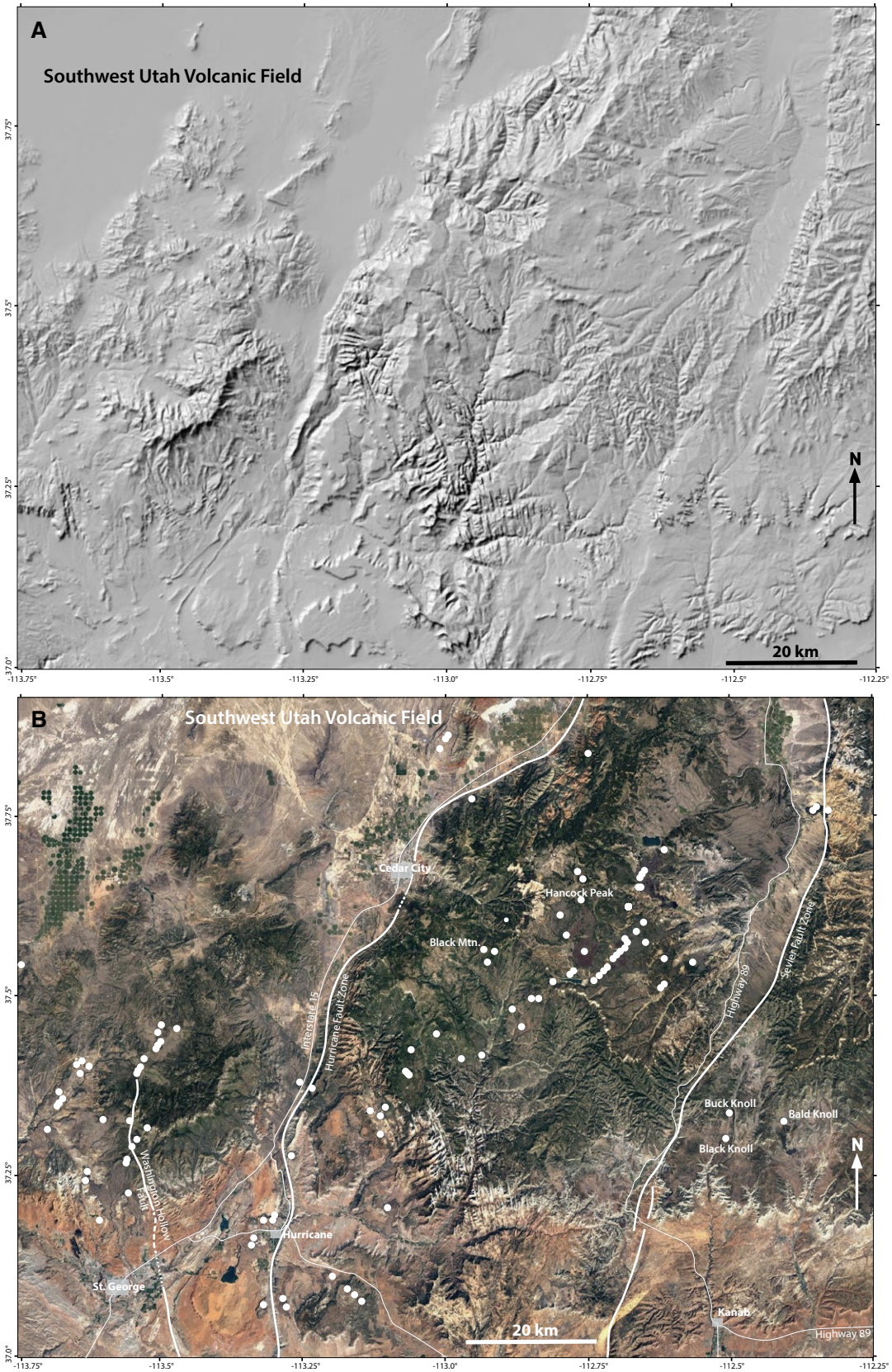

Figure 9. (A) Shaded relief map shows the Southwest Utah volcanic field (from U.S. Geological Survey site https://apps.nationalmap.gov/3depdem). (B) Google Earth image of the area of the Southwest Utah volcanic field. The towns of St. George, Kanab, and Cedar City are indicated, and some cones that are called out in the literature are named. White dots indicate scoria cones and ramparts based upon maps of Rowley et al. (2006), Doelling (2008), and Biek et al. (2010, 2015). Thin white lines are roads, and thick lines are major normal faults, all of which have downward displacements to the west. Southern edges of the figures correspond to the Utah-Arizona border.

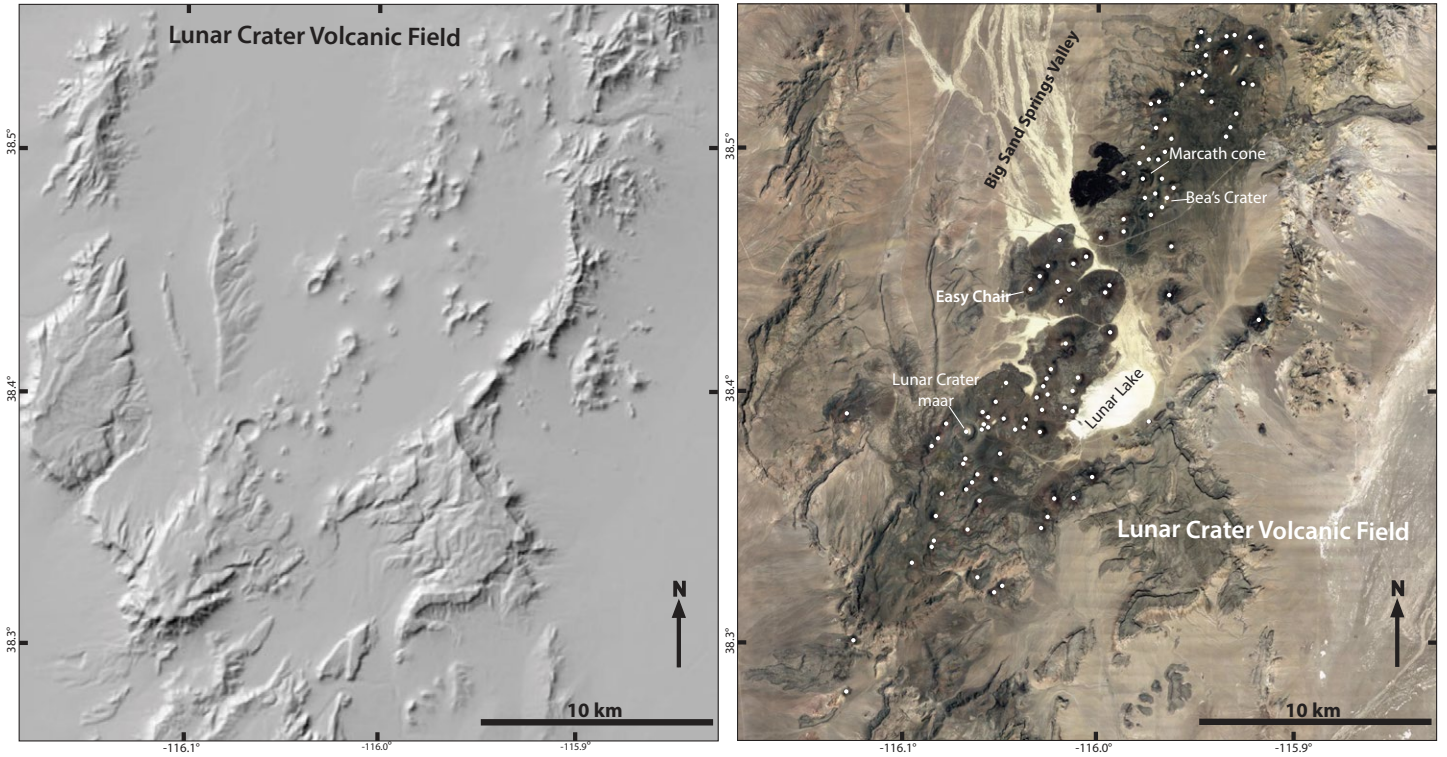

Figure 10. (A) Shaded relief map shows the northern, Quaternary part of the Lunar Crater volcanic field, central Nevada (from U.S. Geological Survey site https://apps.nationalmap.gov/3depdem). (B) Google Earth image of the Quaternary part of the Lunar Crater volcanic field with white dots marking vents (see Tadini et al., 2014; Valentine et al., 2017).

Valentine, 2017). Lunar Crater is the youngest of the maars, and its eruption appears to have been entirely dominated by phreatomagmatic explosions (Valentine et al., 2011, 2017).

The Quaternary volcanoes have compositions of basalts (sensu stricto), trachybasalts, basanites, and tephrites and represent the final two (out of four) magma genesis episodes in the Lunar Crater field (Cortés et al., 2015; Rasoazanamparany et al., 2015; Valentine et al., 2017). Magmas were sourced in enriched asthenosphere and have geochemical signatures similar to those of oceanic-island basalts with indicators of recycled, ancient dehydrated oceanic crust, and hydrous fluids associated with more recent subduction events along the western margin of North America (Rasoazanamparany et al., 2015). This interpretation is consistent with data from deep-seated xenoliths (Bergman et al., 1981). The mantle sources were heterogeneous, with spatial variability at scales of 500 m or less based upon data from closely spaced volcanoes (Rasoazanamparany et al., 2015). Detailed petrologic study of four of the volcanoes indicates that a small degree of partial melting took place at depths of 60–130 km. Magmas stalled just below the base of the crust, where they underwent up to 11% crystallization and then migrated rapidly upward with some magmas stalling a second time at mid-crustal levels, while other magmas simply completed their ascent and erupted at the surface (Cortés et al., 2015). Individual clusters of volcanoes persist over periods of a million years or more, and through different magma genesis episodes, with no evidence of sustained crustal reservoirs between the monogenetic eruptions in the clusters studied (Cortés et al., 2015; Rasoazanamparany et al., 2015; Valentine et al., 2017). Valentine et al. (2017) suggested a potential interplay between surface structures and clusters and deeper magma source and ascent processes.

Pinacate (Sonora, Mexico)

The Pinacate volcanic field is located mostly in Sonora, Mexico, with a few volcanoes on the Arizona side of the international border (Fig. 11, Table 4). The

field contains ~416 Quaternary vents (Lutz and Gutmann, 1995). Topography of the southern portion of the field is dominated by the Santa Clara shield volcano (1.7–1.1 Ma; Fig. 11), a polygenetic volcano whose products are related to each other through a differentiation series featuring early basanite through a small volume of late-stage trachyte (Lynch et al., 1993). Santa Clara volcano is mantled by cones and lavas of the younger (post-1.2 Ma) Pinacate series of monogenetic basaltic volcanoes (Lynch et al., 1993; García-Abdeslem and Calmus, 2015), which also extend northward and contribute to the full footprint of the volcanic field. Because volcanological research has been sparse relative to the number of volcanoes, it is not known how many of the 416 vents record separate monogenetic events; based upon imagery, it seems likely that many such events produced multiple vents.

The Pinacate field contains a typical range of volcanic landforms from scoria cones to agglomerate ramparts, with evidence of Hawaiian to Strombolian to

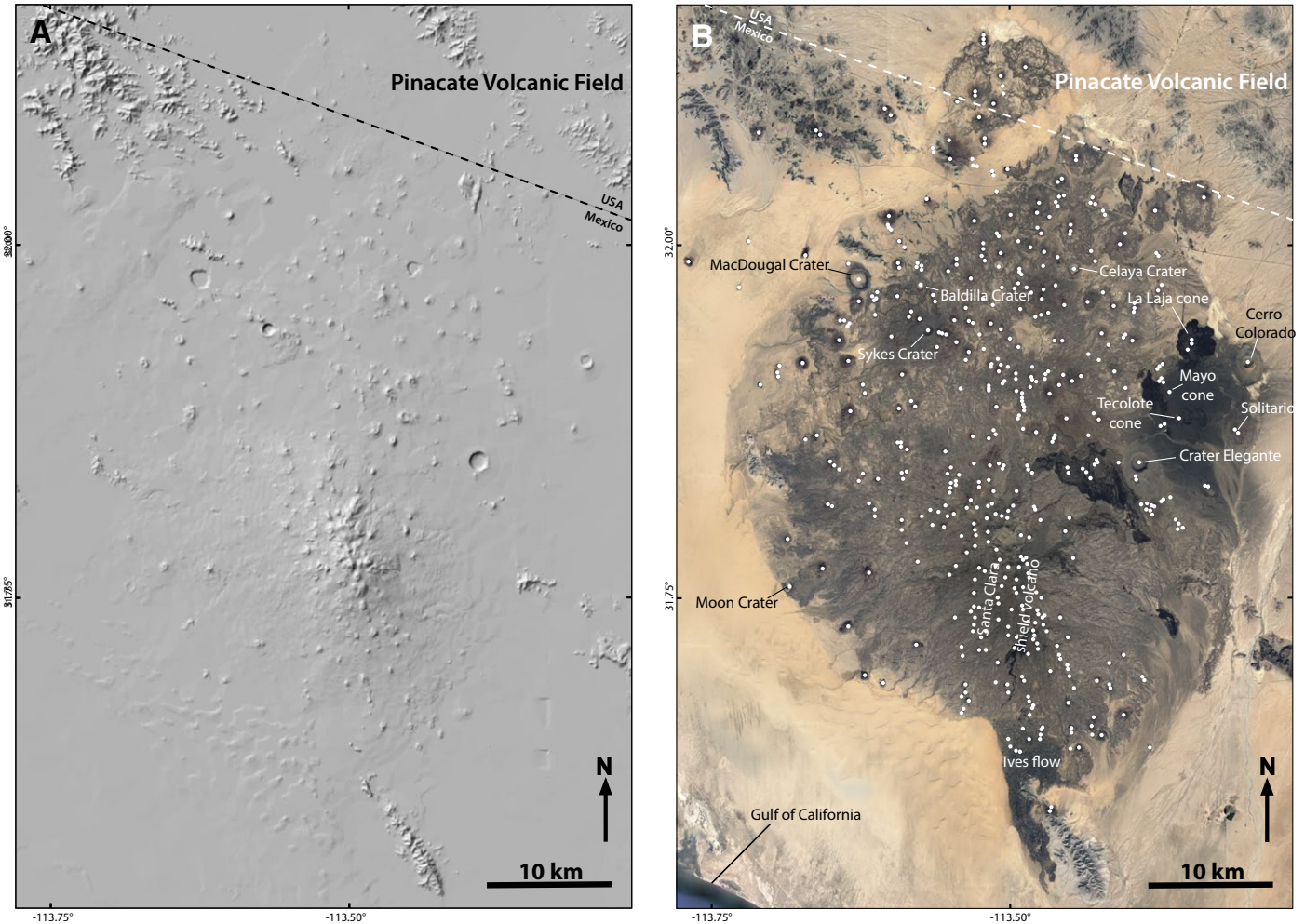

Figure 11. (A) Shaded relief map shows the Pinacate volcanic field, which is mostly in Sonora, Mexico (from U.S. Geological Survey site https://apps.nationalmap.gov/3depdem). (B) Google Earth image of the Quaternary Pinacate volcanic field with white dots mark venting discernable on imagery. Santa Clara shield volcano in the southern part of the field dates to 1.7–1.1 Ma, while the bulk of the volcanoes are younger (García-Abdeslem and Calmus, 2015).

violent Strombolian explosive eruptions and associated pyroclastic deposits, and a variety of lava morphologies (Gutmann, 1979; Zawacki et al., 2019). Many cones and lava fields demonstrate evidence of cone failure and rafting processes. The approximately 10 maar volcanoes have diameters ranging from ~270 m to 1.6 km. Two of these maars have been the subject of physical volcanological studies focusing on phreatomagmatic processes (Wohletz and Sheridan, 1983), evidence for switching between phreatomagmatic and magmatic volatile-driven mechanisms (Gutmann, 1979, 2002), and pyroclastic surge facies (Wohletz and Sheridan, 1979). Lutz and Gutmann (1995) quantified vent alignments in the volcanic field and determined that older vents produce alignments of ~N10°E, which is roughly parallel to Basin-and-Range extensional structures in the area, while vents younger than ca. 400 ka also exhibit alignments oriented ~N20°W (similar to the elongate axis of the Santa Clara shield volcano) and ~N55°W. They inferred that the latter orientation may reflect decreased differential stresses in the crust or increased magma pressure in ascending dikes, or a combination of both, which allowed the dikes to align parallel to a late Miocene detachment fault that may extend into the volcanic field.

There is no systematic trend in composition with age or location amongst the Pinacate series volcanoes (Lynch et al., 1993), although it is worth noting that only a small fraction of them have been characterized geochemically (Lynch's 1981 dissertation contains geochemical data for 13 Pinacate series samples, but the 1993 paper cited here is the only widely accessible publication that we were able to find; it reports data for three of the monogenetic volcanoes). Compositions are mainly alkali basalts to trachybasalts, although the voluminous Ives lava flow (southern part of the field; Fig. 11) is tholeiitic. Lynch et al. (1993) concluded that the magmas were generated in the asthenosphere by varying degrees of partial melting of an oceanic island or enriched mid-oceanic ridge source; they found no evidence that the Pinacate magmas are influenced by the Gulf of California spreading center some 100 km to the southwest, and this conclusion was also supported by Zawacki et al. (2019).

REGIONAL SCALE RECURRENCE RATES AND ANNUAL PROBABILITIES

Compilation of the total Quaternary volcano count and age data allows a first-order estimate of the recurrence rate (or interval) of basaltic volcanism on the scale of the entire Southwest. To the extent that we could determine, only ~25% of the Quaternary basaltic volcanoes have been dated, although this percentage is somewhat uncertain because of the potential volcano overcount/undercount (see Section 4) and because in some cases we were not able to determine whether multiple dates belonged to the same individual centers. Of the 548 volcanoes for which dates were compiled (Table S1 [footnote 1]), 225 are based only on the K-Ar method, which, especially for whole-rock analyses published in earlier literature, tends to overestimate ages of young basalts. Note that both of these numbers (548 dated volcanoes and 225 dated only by K-Ar) may be artificially high by ~20 ages, as some of the Cima K-Ar ages are likely from multiple samples of individual cones/flows (Table S1). We do not imply that all K-Ar ages in our compilation are suspect, and it is beyond the scope of our study to conduct a detailed assessment of this issue. However, a modern approach to geochronology of Quaternary basalts would more heavily rely on the $^{40}Ar/^{39}Ar$ method (e.g., Heizler et al., 1999) and on cosmogenic surface-exposure techniques (e.g., Shepard et al., 1995; Dunbar and Phillips, 2004); by our count, these methods have been applied to only ~15% of the Quaternary volcanoes in the Southwest. Our estimate of regional recurrence interval does not filter out these issues of volcano versus vent counts, and older versus newer geochronological methods, but is intended to provide a starting point from which decisions about further data collection could be made.

Recent decades have seen advances in the application of probabilistic methods to volcanoes and volcanic fields with the degree of sophistication corresponding to the completeness of the volcano count, geochronological, and spatial distribution data sets (e.g., Dzierma and Wehrmann, 2010a, 2010b; Wehrmann and Dzierma, 2011; Marzocchi and Bebbington, 2012; Bebbington, 2013; Bevilacqua et al., 2018). Our sparse data coverage (only 25% of volcanoes dated) across many widely separated volcanic fields that likely operate independently of each other justifies the use of a simple Poisson model for temporal eruption probabilities for the Southwest as a whole. The Poisson model assumes a constant mean rate of eruptions, which is appropriate given insufficient data to suggest otherwise (realizing that within individual volcanic fields, and potentially at the regional scale, more data would likely indicate some degree of temporal clustering or episodicity) and that each eruption is independent (see below). Such a model has been used in volcanology at least since Crowe et al. (1982), who applied it to the inherently sparse data set of the Quaternary part of the Southwest Nevada volcanic field as part of volcanic hazards assessment for the proposed radioactive waste repository at nearby Yucca Mountain. That work was followed by the application of Poisson models accounting for spatial-temporal clustering of volcanoes in that field (Connor and Hill, 1995; Ho and Smith, 1998). We do not include a spatial-temporal clustering analysis here.

To apply the Poisson approach, monogenetic events as a function of time must fulfill three conditions, as summarized by Dzierma and Wehrmann (2010a; see also Evans et al., 2000). First, events are seldom, such that the probability of an event occurring in a small increment of time is negligible. This can also be articulated by saying that the number of events occurs during non-overlapping time intervals, and the probability of two or more events occurring at the same time is negligible if the window of time is small enough. This condition can be readily accepted based on the time frame of the Quaternary period compared to the total number of events and the duration of activity at a given monogenetic volcano (days to decades). Second, events are independent of each other, meaning the event probability in any time interval is independent of any occurrences before the start time of the interval, and the distribution of the number of events only depends on the length of the interval. This condition is consistent with a definition wherein each monogenetic volcano records a

single and independent eruptive episode. A detailed analysis within an individual volcanic field, with sufficient geochronological data, may show that this condition can be violated, but our focus is on the Southwest as a whole, and given the sparse age data and the broad geographic area, we argue that independence between monogenetic events is reasonable for this first-cut analysis.

The third condition is that the time series is stationary, so there is no time trend that modifies the frequency of the events. Here we use the full age data set (Table S1 [footnote 1]) to assess whether this condition is met. For volcanoes that have multiple age dates, we use their median age. This simple approach is easy to apply consistently and avoids any subjective judgement of preferred ages on our part; we anticipate that the differences that would occur from another age selection method have only minor effects on our analysis below. The frequency of dated events increases with younger ages, which is inconsistent with a Poisson model based upon the full age data set. Although we cannot discard the possibility of changes in the true eruption rate over time, at least some component, and probably most, of this observation is related to the fact that the record—both geological and in terms of age analyses—becomes less complete with increasing age; it is well-known that this type of data set typically has a strong bias toward younger ages (e.g., Brown et al., 2014). By calculating the slope of a cumulative curve using a shifting window of 10 ages, we identify three breaks in the rate at 2.17 Ma, 1.13 Ma, and 720 ka (Fig. 12A). We focus on younger ages as they are likely to be more representative of the overall eruptive rate, specifically a subset of 270 ages that are younger than 720 ka, for which the cumulative age follows a relatively linear trend. Calculating the autocorrelation function of this reduced data set (Fig. 12B; see Varley et al., 2006) shows that it exhibits stationary behavior (i.e., values drop down quickly and stay within a confidence value of ~0.12), which suggests that the subset can be treated as a Poisson process.

For a discrete random variable X that follows a Poisson distribution, the probability of having k events with an average frequency of events λ (events/time) is equal to:

$$P(X = k) = \frac{e^{-\lambda t}(\lambda t)^k}{k!}, \quad (1)$$

where λt is the expected number of occurrences in the given time t. From the reduced data set there are 270 dated events for 720,000 years or 375 events per Ma. The frequency of the dated events is therefore $\lambda = 3.75 \times 10^{-4}$ yr^{-1} or one eruption every 2667 years, which is comparable with the average repose time between events (~4798 years), across the entire Southwest. These results support a stationary process for the subset and allow modeling of the repose time as a Poisson process. Using λ in Equation 1 yields a recurrence rate for the formation of a new monogenetic basaltic volcano as:

$$P(X = 1) = e^{-3.75\times10^{-4}} \times 3.75 \times 10^{-4}\,\text{yr}^{-1} = 3.74 \times 10^{-4}\,\text{yr}^{-1}. \quad (2)$$

Longer time windows (Table 5) yield larger probabilities for one event during the window if the time is less than ~2667 years (for example, over a

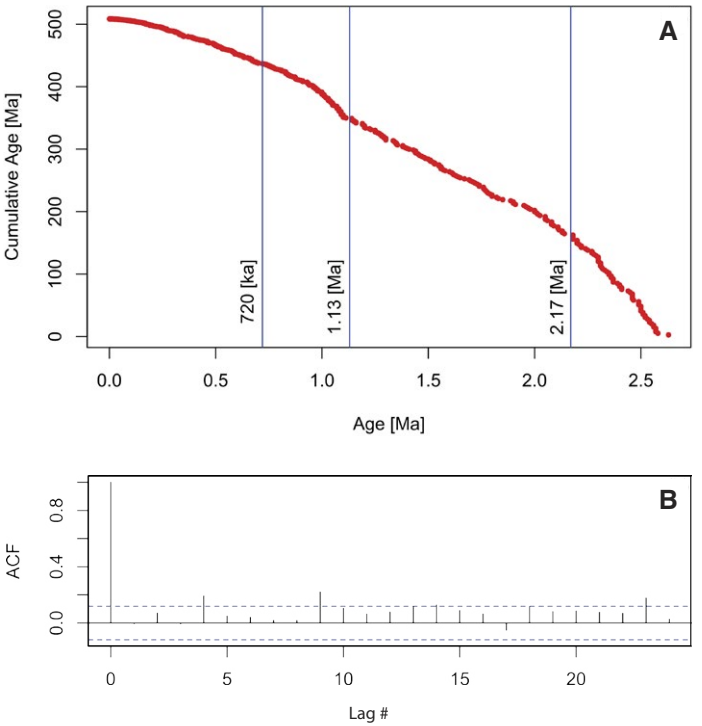

Figure 12. (A) Cumulative age for all dated volcanoes is plotted (Table S1 [see footnote 1]). Blue bars show changes in rates as defined by the age data. (B) Autocorrelation function for a subset of the geochronology data set that represents volcanoes with ages of less than 720 ka.

1000 yr time window, there is a 0.258 or 0.364 probability of a new monogenetic volcano in the region depending upon whether the <720 ka portion of the data set is used or the full volcano count as described below), while times exceeding that value yield smaller probabilities as it becomes increasingly less likely to have only one eruption during the time window. We emphasize that the recurrence rate and probability are likely artificially low due to the fact that they are only based on dated events.

Uncertainty in events is a result of a gap between the actual occurrences and the availability of knowledge regarding the events in addition to other factors such as analytical uncertainties in age determinations. To compare the recurrence rates and probabilities of dated events (<720 ka) with those of the actual occurrences, we now calculate the recurrence rate of a new volcano with a rate based on the total 2229 *observed* monogenetic volcanoes (both dated and undated, and assuming they are uniformly distributed in time at the regional scale and with the data at hand; Table S1) in 2.58 Ma, which is 864 events per Ma ($\lambda = 8.64 \times 10^{-4}$ yr^{-1}). With this information, the recurrence rate is:

TABLE 5. PROBABILITY OF ONE ERUPTION FOR DIFFERENT TIME WINDOWS

Time window (years)	Probability based upon ages <720 ka	Probability based on total volcano count
1	3.74×10^{-4}	8.63×10^{-4}
100	3.6×10^{-2}	7.92×10^{-2}
1000	0.258	0.364
2667	0.368	0.230
5000	0.288	5.7×10^{-2}
10,000	0.088	1.53×10^{-3}

$$P(X=1) = e^{-8.64\times10^{-4}} \times 8.64\times10^{-4}\,\mathrm{yr}^{-1} = 8.63\times10^{-4}\,\mathrm{yr}^{-1}, \quad (3)$$

which is more than twice as large as the rate based only on dated volcanoes with ages less than 720 ka. The difference in results of Equations 2 and 3 gives an indication of the large degree of uncertainty that arises from the sparse data coverage. It does not account for the additional uncertainties due to buried volcanoes and to potential co-eruptive vents having been counted as individual volcanoes.

The time for the next event with probability P given that an amount of time t has occurred since the last eruption is equivalent to asking for no event during the time window ($k = 0$). This reduces Equation (1) to:

$$P(k=0) = \frac{e^{-\lambda t} \times (\lambda t)^0}{0!} = e^{-\lambda t}, \quad (4)$$

and rearranging yields:

$$t = -\frac{ln\ P}{\lambda}. \quad (5)$$

Assuming $\lambda = 3.75 \times 10^{-4}$ yr^{-1}, a time of ~137 years has a 95% chance of not having an eruption, while a time of ~1028 years has a 68% chance of not having an eruption, when only the dated, <720 ka volcanoes are used. For comparison, using the full volcano count ($\lambda = 8.63 \times 10^{-4}$ yr^{-1}) in a time frame of ~60 years, there is a 95% chance of not having an eruption, while in an interval of ~450 years there is a 68% chance of having an eruption.

DISCUSSION

Basaltic volcanic fields are widely dispersed across the American Southwest, though they are more abundant close to the boundaries between provinces; however, with one exception (Pinacate), the seven major fields described above form a broad, northwest-trending band of intensive Quaternary basaltic volcanism (Fig. 13). Four of the fields (Springerville, San Francisco, Uinkaret, and SW Utah) are close to the transition between the Colorado Plateau and Basin and Range Provinces, while three of them (Potrillo, Geronimo-San Bernardino, and Lunar Crater) are well within the Basin and Range Province. Volcanism along the Plateau margin has received significant attention from a petrogenetic and geodynamic perspective, and melt production mechanisms are typically tied to the increase in lithospheric thickness at the transition from the Basin and Range to the Colorado Plateau, which, for example, may result in delamination processes with associated upwelling (Table 3). On the other hand, volcanism within the Basin and Range (including the Rio Grande Rift) is typically attributed to extension-related upwelling (Table 3).

The band of major fields may be a coincidence, but it is roughly parallel to major dextral shear zones related to relative motion between the North American and Pacific tectonic plates (Fig. 13). The dominantly transpressional San Andreas fault system is well known to most geologists and accommodates much of the strain induced by the relative motion, but shear deformation extends into the continent including the transtensional Walker Lane-Eastern California Shear Zone along the western edge of the Basin and Range Province. This transtensional belt takes up ~20% of the strain caused by relative plate motion (Carlson et al., 2013). GPS network data indicate that plate boundary shear plays an important role in active deformation as far as 800 km inboard from the plate boundary (Hammond et al., 2014). Recent structural geology work in western and central Arizona indicates that Neogene faulting there is influenced by relative plate motion, which indicates that plate boundary stresses are distributed well into the Southwest (Singleton et al., 2019). We suggest that small amounts of shear strain due to the dextral relative motion at the Pacific-North America boundary may play a role in development of the band of major volcanic fields. Shear deformation can focus very small fractions of partial melt (e.g., Holtzman and Kohlstedt, 2007) and has been suggested as a mechanism for collecting melt even in non-convecting lithospheric mantle (Valentine and Perry, 2007) as well as asthenospheric mantle (Katz et al., 2006; Holtzman and Kohlstedt, 2007; Valentine and Hirano, 2010; Valentine et al., 2017). We do not suggest such shear-focusing as the only, or even main, driver for magmatism in these fields, but it may augment other geodynamic mechanisms (Table 3) in controlling the locations of the major fields and enhancing their magma production.

Another band of volcanic fields, the Jemez lineament, stretches northeast from the Springerville field at its southwestern end to the Raton-Clayton field (Fig. 13). Although these fields have had less Quaternary activity than the major fields discussed above, it is noteworthy that some of the most recent activity in the Southwest, and farthest inboard from plate boundaries, has occurred on this lineament (e.g., the ca. 3 ka McCartys flow in the Zuni-Bandera field). The Jemez lineament coincides with a suture between two Proterozoic crustal provinces (summarized by Nereson et al., 2013), which has been inferred to provide a fertile source for melting and a pathway for magmas to the surface. In our view, the detailed mechanisms for magmatism along the Jemez Lineament remain largely unknown.

Although we focus on basaltic volcanism, a few of the Southwestern fields (Fig. 1) are associated with substantial volumes of intermediate to silicic eruptive products. The Cerros del Rio field (New Mexico) is peripheral to the

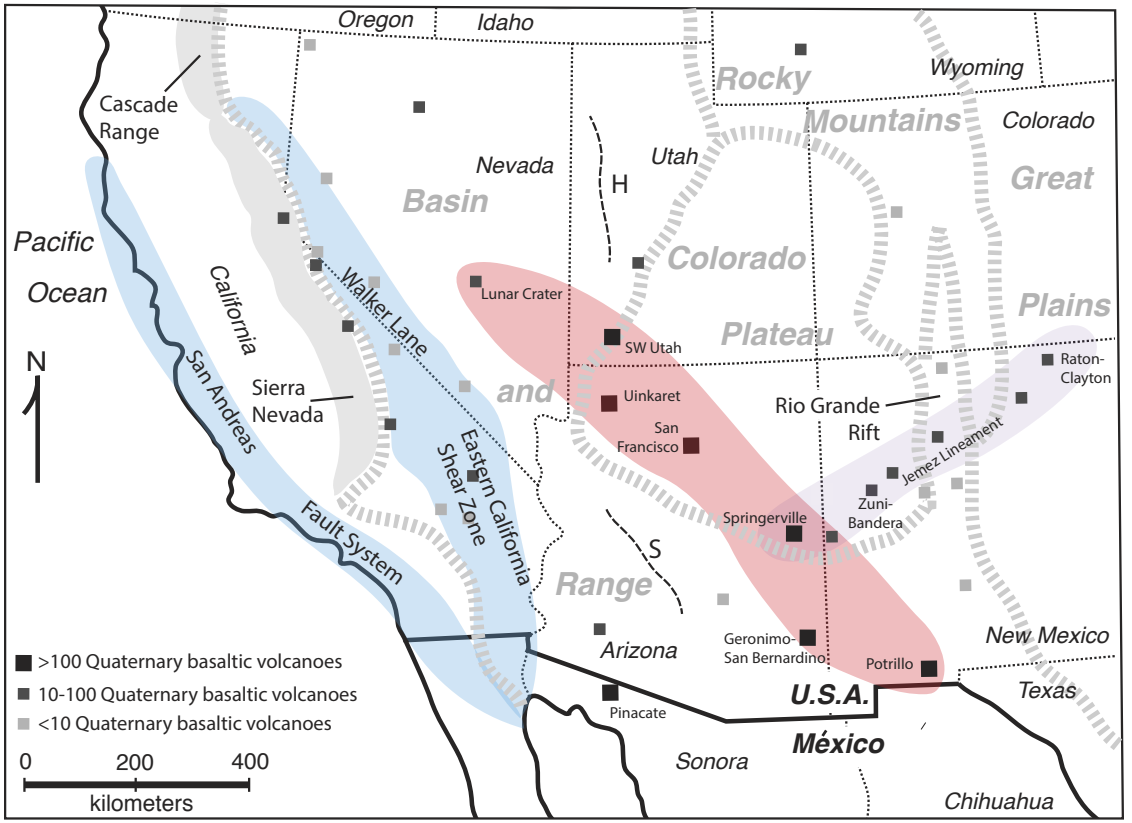

Figure 13. Quaternary basaltic volcanic field locations and relative sizes are shown (in terms of vent/volcano counts), simplified from Figure 1. Red band encloses the major volcanic fields (>100 Quaternary vents; see Section 5.7 for rationale of including Lunar Crater field, which has just under 100 mappable vents), and shows a NW-SE trend that is roughly parallel to major dextral shear zones to the west (San Andreas fault system is transpressional, while Walker Lane-Eastern California Shear Zone is transtensional; zones are based on Wesnousky, 2005; Faulds et al., 2005; Putirka and Busby, 2011). Dashed lines labeled H and S show approximate inboard extent of plate boundary-related dextral motion from GPS data (Hammond et al., 2014) and structural analysis (Singleton et al., 2019), respectively. Light purple band indicates Jemez lineament.

larger Jemez volcanic field, which produced hundreds of cubic kilometers of intermediate lavas in late Miocene through Pliocene time (Kelley et al., 2013). Quaternary volcanism there includes two large-volume, silicic, caldera-forming eruptions (Bandelier Tuff), and significant rhyolitic eruptions continued into late Pleistocene time (Self et al., 1986; Wolff et al., 2000, 2005). Basaltic volcanoes in the Mammoth Mountain-Mono-Inyo system (California) occur in an area of intermediate to silicic volcanoes including the Long Valley Caldera and associated Bishop Tuff (e.g., Hildreth et al., 2014). Mount Taylor (New Mexico) basalts surround a composite volcano composed mainly of older, Pliocene trachytic lava domes and flows (Perry et al., 1990; Goff et al., 2019). The San Francisco volcanic field has produced large amounts of intermediate and silicic lavas and tuffs contemporaneously with basaltic volcanism. The field overall is one-half to two-thirds evolved lavas by volume, which are mostly focused on a half-dozen composite centers and a few smaller dome systems (note that dates for evolved centers in this field are included as a separate sheet in Table S1). The evolved magmas in these fields indicate large fluxes of basalt beneath the evolved centers, which are sufficient to alter the thermal and stress fields in the crust enough to maintain long-lived reservoirs and mush zones that repeatedly feed polygenetic eruptive episodes (Cashman et al., 2017). Some of the other basaltic fields, such as Pinacate and the older, Pliocene part of Lunar Crater, contain minor volumes of trachyte domes and flows, which indicates relatively small-scale magma storage and fractionation/assimilation processes of magma batches that are consistent with monogenetic activity. Thus, in places where, and time periods when, magmatism is focused and voluminous, silicic volcanism and associated explosive hazards must be considered when assessing distributed volcanism in the Southwest.

The recurrence rate based only upon dated volcanoes (<720 ka) is equivalent to one volcano on average every ~2700 years, while that based on the total volcano count is equivalent to one volcano every ~1200 years, or every ~960 years for the 52 volcanoes during the last 50 k.y. (Table 2). For comparison, the four

youngest in the Southwest are: Sunset Crater (~900 yr, San Francisco field), Little Springs (~1300 yr and possibly as young as 1025 CE, Uinkaret field), McCartys flow (~3 ka, Zuni-Bandera field), and Dotsero in Colorado (~4150 yr). (Note: Cerro Colorado volcano in the Pinacate field has a magnetic secular variation age of ca. 3.9 ka, but this young age is contradicted by stratigraphic relations.) These four volcanoes all formed within about the last ~4150 years, which is equivalent to one volcano every ~1040 years. This timeframe is too short to be a statistically rigorous comparison for rates estimated over 2.58 m.y., but it is reasonably similar to the full count-based rate given all of the uncertainties. Much more geochronological and physical volcanological work is needed to test whether there are non-Poisson temporal and spatial trends on the regional scale as well as at the scale of individual fields. However, the regional recurrence rates are similar to those at some composite volcanoes, which can have repose periods of hundreds of years or more (McNutt and Roman, 2015; see also Passarelli and Brodsky, 2012). A major complication from a monitoring perspective, compared to the case of a composite volcano, is the large geographic area within which a new monogenetic basaltic volcano may form, along with a potential for only a short period of precursory indicators, such as seismicity, ranging from a year or two to as short as a few weeks (e.g., Albert et al., 2016; Brenna et al., 2018).

CONCLUSION

We have summarized our current understanding of distributed, basaltic monogenetic volcanism in the American Southwest from petrogenetic, volcanological, and geochronological perspectives. A striking observation is that most of the 2229 Quaternary basaltic volcanoes are essentially unstudied beyond the level of detail of regional mapping and limited geochemical and petrologic research that has mostly focused on "big picture" petrogenetic and geodynamic questions. Only 25% of the volcanoes have been dated, and many of those ages were obtained with relatively poorly suited K-Ar methods. Physical volcanological studies have only been conducted on a handful of the volcanoes. Even with the poor coverage of geochronological data, the recurrence rates and annual probabilities indicate that a new monogenetic basaltic eruption, with its attendant hazards, has a likelihood on a regional scale that is commensurate with that of a re-awakening composite volcano such as might be found in the Cascade Range of the Pacific Northwest. We hope that this paper provides a starting point for focused studies to improve our understanding of this important type of volcanism.

ACKNOWLEDGMENTS

G.A. Valentine acknowledges support of previous work on Southwestern basaltic volcanism, some of which is reviewed here, from National Science Foundation (NSF) grants EAR-1420455 and EAR-1016100, the latter of which also supported J.A. Cortés' work. M.H. Ort received funding from NSF grants EAR-0409117, EAR-1156953, and EAR-1322081. We thank Judy Fierstein and Wes Hildreth for reviewing our age data for the Mammoth Mountain-Mono-Inyo field, and Lucy McGee, Wendy Stovall, and editor Shan de Silva for critical reviews of the manuscript that helped to sharpen it.

REFERENCES CITED

Albert, H., Costa, F., and Martí, J., 2016, Years to weeks of seismic unrest and magmatic intrusions precede monogenetic eruptions: Geology, v. 44, p. 211–214, https://doi.org/10.1130/G37239.1.

Alfano, F., Ort, M.H., Pioli, L., Self, S., Hanson, S.L., Roggensack, K., Allison, C.M., Amos, R., and Clarke, A.B., 2019, Sub-Plinian monogenetic basaltic eruption of Sunset Crater, Arizona, USA: Geological Society of America Bulletin, v. 131, p. 661–674, https://doi.org/10.1130/B31905.1.

Amin, J., and Valentine, G.A., 2017, Compound maar crater and co-eruptive scoria cone in the Lunar Crater Volcanic Field (Nevada, USA): Journal of Volcanology and Geothermal Research, v. 339, p. 41–51, https://doi.org/10.1016/j.jvolgeores.2017.05.002.

Arculus, R.J., and Gust, D.A., 1995, Regional petrology of the San Francisco Volcanic Field, Arizona, USA: Journal of Petrology, v. 36, p. 827–861, https://doi.org/10.1093/petrology/36.3.827.

Asmerom, Y., 1999, Th-U fractionation and mantle structure: Earth and Planetary Science Letters, v. 166, p. 163–175, https://doi.org/10.1016/S0012-821X(99)00008-4.

Baldridge, W.S., 2004, Geology of the American Southwest: A Journey through Two Billion Years of Plate-Tectonic History: Cambridge, UK, Cambridge University Press, 280 p, https://doi.org/10.1017/CBO9780511807480.

Ballmer, M.D., Conrad, C.P., Smith, E.I., and Johnsen, R., 2015, Intraplate volcanism at the edges of the Colorado Plateau sustained by a combination of triggered edge-driven convection and shear-driven upwelling: Geochemistry, Geophysics, Geosystems, v. 16, p. 366–379, https://doi.org/10.1002/2014GC005641.

Bebbington, M.S., 2013, Assessing spatio-temporal eruption forecasts in a monogenetic volcanic field: Journal of Volcanology and Geothermal Research, v. 252, p. 14–28, https://doi.org/10.1016/j.jvolgeores.2012.11.010.

Bergman, S.C., Foland, K.A., and Spera, F.J., 1981, On the origin of an amphibole-rich vein in a peridotite inclusion from the Lunar Crater Volcanic Field, Nevada, U.S.A: Earth and Planetary Science Letters, v. 56, p. 343–361, https://doi.org/10.1016/0012-821X(81)90139-4.

Best, M.G., McKee, E.H., and Damon, P.E., 1980, Space-time-composition patterns of late Cenozoic mafic volcanism, southwestern Utah and adjoining areas: American Journal of Science, v. 280, p. 1035–1050, https://doi.org/10.2475/ajs.280.10.1035.

Bevilacqua, A., Bursik, M., Patra, A., Pitman, E.B., Yang, Q., Sangani, R., and Kobs-Nawotniak, S., 2018, Late Quaternary eruption record and probability of future volcanic eruptions in the Long Valley volcanic region (CA, USA): Journal of Geophysical Research: Solid Earth, v. 123, p. 5466–5494, https://doi.org/10.1029/2018JB015644.

Biek, R.F., Rowley, P.D., Hayden, J.M., Hacker, D.B., Willis, G.C., Hintze, L.F., Anderson, R.E., and Brown, K.D., 2010, Geologic map of the St. George and east part of the Colver Mountains 30′ × 60′ quadrangles, Washington and Iron Counties, Utah: Utah Geological Survey Map 242DM, scale 1:100,000, 107 p. text.

Biek, R.F., Moore, D.W., and Nealey, L.D., 2011, Geologic map of the Henrie Knolls quadrangle, Garfield, Kane, and Iron Counties, Utah: Utah Geological Survey Map 252DM, scale 1:24,000, 1 sheet, 1 p. text.

Biek, R.F., Rowley, P.D., Anderson, J.J., Maldonado, F., Moore, D.W., Hacker, D.B., Eaton, J.G., Hereford, R., Sable, E.G., Fikorn, H.F., and Matyjasik, B., 2015, Geologic map of the Panguitch 30′ × 60′ quadrangle, Garfield, Iron, and Kane Counties, Utah: Utah Geological Survey Map 270DM, scale 1:62,500, 3 sheets, 162 p. text.

Biggs, T.H., Leighty, R.S., Skotnicki, S.J., and Pearthree, P.A., 1999, Geology and geomorphology of the San Bernardino Valley, southeastern Arizona: Arizona Geological Survey Open-File Report 99–19, scale 1:32,000, 3 sheets, 20 p. text.

Billingsley, G.H., Hamblin, W.K., Wellmeyer, J.L., and Dudash, S.L., 2001, Geologic map of part of the Uinkaret volcanic field, Mohave County, northwest Arizona: U.S. Geological Survey Miscellaneous Field Studies MF-2368, scale 1:31,680, 1 sheet, 35 p. text.

Brenna, M., Cronin, S.J., Smith, I.E.M., Tollan, P.M.E., Scott, J.M., Prior, D.J., Bamberry, K., and Ukstins, I.A., 2018, Olivine xenocryst diffusion reveals rapid monogenetic basalt ascent following complex storage at Pupuke Maar, Auckland Volcanic Field, New Zealand: Earth and Planetary Science Letters, v. 499, p. 13–22, https://doi.org/10.1016/j.epsl.2018.07.015.

Brown, S.K., Crosweller, H.S., Sparks, R.S.J., Cottrell, E., Deligne, N., Ortiz, N., Hobbs, L., Kiyosugi, K., Loughlin, S., Siebert, L., and Takarada, S., 2014, Characterisation of the Quaternary eruption record: Analysis of the large magnitude explosive volcanic eruptions (LaMEVE) database: Journal of Applied Volcanology, v. 3, p. 5, https://doi.org/10.1186/2191-5040-3-5.

Browne, B., Bursik, M., Deming, J., Louros, M., Martos, A., and Stine, S., 2010, Eruption chronology and petrologic reconstruction of the ca. 8500 yr B.P. eruption of Red Cones, southern

Inyo chain, California: Geological Society of America Bulletin, v. 122, p. 1401–1422, https://doi.org/10.1130/B30070.1.
Brumbaugh, D.S., Hodge, B.E., Linville, L., and Cohen, A., 2014, Analysis of the 2009 earthquake swarm near Sunset Crater volcano, Arizona: Journal of Volcanology and Geothermal Research, v. 285, p. 18–28, https://doi.org/10.1016/j.jvolgeores.2014.07.016.
Bussod, G.Y.A., and Williams, D.R., 1991, Thermal and kinematic model of the southern Rio Grande rift: Inferences from crustal and mantle xenoliths from Kilbourne Hole, New Mexico: Tectonophysics, v. 197, p. 373–389, https://doi.org/10.1016/0040-1951(91)90051-S.
Carlson, C.S., Pluhar, C.J., Glen, J.M.G., and Farner, M.J., 2013, Kinematics of the west-central Walker Lane: Spatially and temporally variable rotations evident in the Late Miocene Stanislaus Group: Geosphere, v. 9, p. 1530–1551, https://doi.org/10.1130/GES00955.1.
Cashman, K.V., Sparks, R.S.J., and Blundy, J.D., 2017, Vertically extensive and unstable magmatic systems: A unified view of igneous processes: Science, v. 355, no. eaag3055, https://doi.org/10.1126/science.aag3055.
Christiansen, R.L., and Lipman, P.W., 1972, Cenozoic volcanism and plate-tectonic evolution of the Western United States. II. Late Cenozoic: Philosophical Transactions of the Royal Society of London A: Mathematical, Physical, and Engineering Sciences, v. 271, p. 249–284.
Cipar, J.H., Garber, J.M., Kylander-Clark, A.R.C., and Smye, A.J., 2020, Active crustal differentiation beneath the Rio Grande Rift: Nature Geoscience, v. 13, p. 75, https://doi.org/10.1038/s41561-020-0640-z.
Condit, C., 2010, Dynamic Digital Map of the Springerville Volcanic Field and the DDM-Template: An example of an open-source tool to distribute maps, data, articles, and multi-media materials: Geosphere, v. 6, no. 4, p. 430–443, https://doi.org/10.1130/GES00531.1.
Condit, C., and Connor, C.B., 1996, Recurrence rates of volcanism in basaltic volcanic fields: An example from the Springerville volcanic field, Arizona: Geological Society of America Bulletin, v. 108, p. 1225–1241, https://doi.org/10.1130/0016-7606(1996)108<1225:RROVIB>2.3.CO;2.
Condit, C., Crumpler, L., Aubele, J., and Elston, W., 1989, Patterns of volcanism along the southern margin of the Colorado Plateau: The Springerville field: Journal of Geophysical Research: Solid Earth, v. 94, p. 7975–7986, https://doi.org/10.1029/JB094iB06p07975.
Connor, C.B., and Hill, B.E., 1995, Three nonhomogeneous Poisson models for the probability of basaltic volcanism: Application to the Yucca Mountain region, Nevada: Journal of Geophysical Research: Solid Earth, v. 100, p. 10,107–10,125, https://doi.org/10.1029/95JB01055.
Conrad, C.P., Wu, B., Smith, E.I., Bianco, T.A., and Tibbetts, A., 2010, Shear-driven upwelling induced by lateral viscosity variations and asthenospheric shear: A mechanism for intraplate volcanism: Physics of the Earth and Planetary Interiors, v. 178, p. 162–175, https://doi.org/10.1016/j.pepi.2009.10.001.
Conway, F.M., Ferrill, D.A., Hall, C.M., Morris, A.P., Stamatakos, J.A., Connor, C.B., Halliday, A.N., and Condit, C., 1997, Timing of basaltic volcanism along the Mesa Butte Fault in the San Francisco Volcanic Field, Arizona, from $^{40}Ar/^{39}Ar$ dates: Implications for longevity of cinder cone alignments: Journal of Geophysical Research: Solid Earth, v. 102, p. 815–824, https://doi.org/10.1029/96JB02853.
Conway, F.M., Connor, C.B., Hill, B.E., Condit, C.D., Mullaney, K., and Hall, C.M., 1998, Recurrence rates of basaltic volcanism in SP cluster, San Francisco volcanic field, Arizona: Geology, v. 26, p. 655–658, https://doi.org/10.1130/0091-7613(1998)026<0655:RROBVI>2.3.CO;2.
Cortés, J.A., Smith, E.I., Valentine, G.A., Johnsen, R., Rasoazanamparany, C., Widom, E., Sas, M., and Ruth, D., 2015, Intrinsic conditions of magmas from the Lunar Crater Volcanic Field (Nevada): Implications for internal plumbing and magma ascent: The American Mineralogist, v. 100, p. 396–413, https://doi.org/10.2138/am-2015-4812.
Cousens, B.L., Wetmore, S., and Henry, C.D., 2013, The Plio-Quaternary Buffalo Valley volcanic field, Nevada: Post-extension, intraplate magmatism in the north-central Great Basin, USA: Journal of Volcanology and Geothermal Research, v. 268, p. 17–35, https://doi.org/10.1016/j.jvolgeores.2013.10.006.
Crow, R., Karlstrom, K., Asmerom, Y., Schmandt, B., Polyak, V., and DuFrane, S.A., 2011, Shrinking of the Colorado Plateau via lithospheric mantle erosion: Evidence from Nd and Sr isotopes and geochronology of Neogene basalts: Geology, v. 39, p. 27–30, https://doi.org/10.1130/G31611.1.
Crow, R.S., Karlstrom, K.E., McIntosh, W., Peters, L., Crossey, L., and Eyster, A., 2015, A new model for Quaternary lava dams in Grand Canyon based on $^{40}Ar/^{39}Ar$ dating, basalt geochemistry, and field mapping: Geosphere, v. 11, no. 5, p. 1305–1342, https://doi.org/10.1130/GES01128.1.
Crowe, B.M., and Fisher, R.V., 1973, Sedimentary structures in base-surge deposits with special reference to cross-bedding, Ubehebe Craters, Death Valley, California: Geological Society of America Bulletin, v. 84, p. 663–682, https://doi.org/10.1130/0016-7606(1973)84<663:SSIBDW>2.0.CO;2.
Crowe, B.M., Johnson, M.E., and Beckman, R.J., 1982, Calculation of the probability of volcanic disruption of a high-level radioactive waste repository within southern Nevada, USA: Radioactive Waste Management and the Nuclear Fuel Cycle, v. 3, p. 167–190.
De Hon, R.A., and Earl, R.A., 2018, Reassessment of features in the Aden Crater lava flows, Doña Ana County, New Mexico: New Mexico Geology, v. 40, p. 17–26.
Delaney, P.T., and Gartner, A.E., 1997, Physical processes of shallow mafic dike emplacement near the San Rafael Swell, Utah: Geological Society of America Bulletin, v. 109, p. 1177–1192, https://doi.org/10.1130/0016-7606(1997)109<1177:PPOSMD>2.3.CO;2.
Doelling, H.H., 2008, Geologic map of the Kanab 30′ × 60′ quadrangle, Kane and Washington Counties, Utah, and Coconino and Mohave Counties, Arizona: Utah Geological Survey Miscellaneous Publication 08–2DM, scale 1:100,000, 1 sheet, 1 p. text.
Duffield, W., Riggs, N.R., Kaufmann, D., Champion, D., Fenton, C.R., Forman, S., McIntosh, W.C., Hereford, R., Plescia, J., and Ort, M., 2006, Multiple constraints on the age of a Pleistocene lava dam across the Little Colorado River at Grand Falls, Arizona: Geological Society of America Bulletin, v. 118, p. 421–429, https://doi.org/10.1130/B25814.1.
Dunbar, N.W., 2005, Quaternary volcanism in New Mexico, *in* Lucas, S.G., Morgan, G.S., and Zeigler, K.E., eds., New Mexico's Ice Ages: New Mexico Museum of Natural History and Science Bulletin 28, p. 95–106.
Dunbar, N.W., and Phillips, F.M., 2004, Cosmogenic ^{36}Cl ages of lava flows in the Zuni-Bandera volcanic field, north-central New Mexico, U.S.A: New Mexico Bureau of Geology and Mineral Resources Bulletin, v. 160, p. 309–317.
Dzierma, Y., and Wehrmann, H., 2010a, Statistical eruption forecast for the Chilean Southern Volcanic Zone: Typical probabilities of volcanic eruptions as baseline for possibly enhanced activity following the large 2010 Concepción earthquake: Natural Hazards and Earth System Sciences, v. 10, p. 2093–2108, https://doi.org/10.5194/nhess-10-2093-2010.
Dzierma, Y., and Wehrmann, H., 2010b, Eruption time series statistically examined: Probabilities of future eruptions at Villarrica and Llaima Volcanoes, Southern Volcanic Zone, Chile: Journal of Volcanology and Geothermal Research, v. 193, p. 82–92, https://doi.org/10.1016/j.jvolgeores.2010.03.009.
Elson, M.D., Ort, M.H., Sheppard, P.R., Samples, T.L., Anderson, K.C., May, E.M., and Street, D.J., 2011, Sunset Crater Volcano, *in* Elson, M.D., ed., Sunset Crater Archaeology: The History of a Volcanic Landscape. Prehistoric Settlement in the Shadow of the Volcano: Tucson, Arizona, USA, Center for Desert Archaeology, Anthropological Papers No. 37, p. 103–129.
Erlund, E.J., Cashman, K.V., Wallace, P.J., Pioli, L., Rosi, M., Johnson, E., and Delgado Grenados, H., 2010, Compositional evolution of magma from Parícutin Volcano, Mexico: The tephra record: Journal of Volcanology and Geothermal Research, v. 197, p. 167–187, https://doi.org/10.1016/j.jvolgeores.2009.09.015.
Evans, M., Hastings, N., and Peacock, B., 2000, Statistical Distributions (3rd edition): New York, John Wiley & Sons, Inc., 221 p.
Farmer, G.L., Perry, F.V., Semken, S., Crowe, B., Curtis, D., and DePaolo, D.J., 1989, Isotopic evidence on the structure and origin of subcontinental lithospheric mantle in southern Nevada: Journal of Geophysical Research: Solid Earth, v. 94, p. 7885–7898, https://doi.org/10.1029/JB094iB06p07885.
Farmer, G.L., Fritz, D.E., and Glazner, A.F., 2020, Identifying metasomatized continental lithospheric mantle involvement in Cenozoic magmatism from Ta/Th values, southwestern North America: Geochemistry, Geophysics, Geosystems, v. 21, https://doi.org/10.1029/2019GC008499.
Faulds, F.E., Henry, C.D., and Hinz, N.H., 2005, Kinematics of the northern Walker Lane, an incipient transform fault along the Pacific-North America plate boundary: Geology, v. 33, p. 505–508, https://doi.org/10.1130/G21274.1.
Fenton, C.R., Webb, R.H., Pearthree, P.A., Cerling, T.E., and Poreda, R.J., 2001, Displacement rates on the Toroweap and Hurricane faults: Implications for Quaternary downcutting in Grand Canyon: Geology, v. 29, p. 1035–1038, https://doi.org/10.1130/0091-7613(2001)029<1035:DROTTA>2.0.CO;2.
Fenton, C.R., Mark, D.F., Barfod, D.N., Niedermann, S., Goethals, M.M., and Stuart, F.M., 2013, $^{40}Ar/^{39}Ar$ dating of the SP and Bar Ten lava flows AZ, USA: Laying the foundation for the SPICE cosmogenic nuclide production-rate calibration project: Quaternary Geochronology, v. 18, p. 158–172, https://doi.org/10.1016/j.quageo.2013.01.007.
Fierstein, J., and Hildreth, W., 2017, Eruptive history of the Ubehebe Crater cluster, Death Valley, California: Journal of Volcanology and Geothermal Research, v. 335, p. 128–146, https://doi.org/10.1016/j.jvolgeores.2017.02.010.
Fisher, R.V., and Waters, A.C., 1970, Base surge bed forms in maar volcanoes: American Journal of Science, v. 268, p. 157–180, https://doi.org/10.2475/ajs.268.2.157.

García-Abdeslem, J., and Calmus, T., 2015, A 3-D model of crustal magnetization at the Pinacate Volcanic field, NW Sonora, Mexico: Journal of Volcanology and Geothermal Research, v. 301, p. 29–37, https://doi.org/10.1016/j.jvolgeores.2015.05.001.

Gazel, E., Plank, T., Forsyth, D.W., Bendersky, C., Lee, C.-T.A., and Hauri, E.H., 2012, Lithospheric versus asthenospheric mantle sources at the Big Pine Volcanic Field, California: Geochemistry, Geophysics, Geosystems, v. 13, article no. Q0AK06, https://doi.org/10.1029/2012GC004060.

Genareau, K., Valentine, G.A., Moore, G., and Hervig, R.L., 2010, Mechanisms for transition in eruptive style at a monogenetic scoria cone revealed by microtextural analyses (Lathrop Wells volcano, Nevada, U.S.A.): Bulletin of Volcanology, v. 72, p. 593–607, https://doi.org/10.1007/s00445-010-0345-z.

Germa, A., Koebli, D., Wetmore, P., Atlas, Z., Arias, A., Savov, I.P., Diez, M., Greaves, V., and Gallant, E., 2020, Crystallization and segregation of syenite in shallow mafic sills: Insights from San Rafael subvolcanic field, Utah: Journal of Petrology, v. 61, no. egaa092, https://doi.org/10.1093/petrology/egaa092.

Gilbert, H., 2012, Crustal structure and signatures of recent tectonism as influenced by ancient terranes in the western United States: Geosphere, v. 8, p. 141–157, https://doi.org/10.1130/GES00720.1.

Goff, F., Kelley, S.A., Goff, C.J., McGraw, D.J., Osburn, G.R., Lawrence, J.R., Drakos, P.G., and Skotnicki, S.J., 2019, Geologic map of the Mount Taylor volcano area, New Mexico: New Mexico Bureau of Geology and Mineral Resources, Geologic Map 80, scale 1:36,000, 1 sheet, 66 p. text.

Gutmann, J.T., 1979, Structure and eruptive cycle of cinder cones in the Pinacate volcanic field and the controls of Strombolian activity: The Journal of Geology, v. 87, p. 448–454, https://doi.org/10.1086/628432.

Gutmann, J.T., 2002, Strombolian and effusive activity as precursors to phreatomagmatism: Eruptive sequence at maars of the Pinacate volcanic field, Sonora, Mexico: Journal of Volcanology and Geothermal Research, v. 113, p. 345–356, https://doi.org/10.1016/S0377-0273(01)00265-7.

Hamblin, W.K., Damon, P.E., and Bull, W.B., 1981, Estimates of vertical crustal strain rates along the western margins of the Colorado Plateau: Geology, v. 9, p. 293–298, https://doi.org/10.1130/0091-7613(1981)9<293:EOVCSR>2.0.CO;2.

Hamilton, C.W., Scheidt, S.P., Sori, M.M., de Wet, A.P., Bleacher, J.E., Mouginis-Mark, P.J., Self, S., Zimbelman, J.R., Garry, W.B., Whelley, P.L., and Crumpler, L.S., 2020, Lava-rise plateaus and inflation pits in the McCartys lava flow field, New Mexico: An analog for Pāhoehoe-lava flows on planetary surfaces: Journal of Geophysical Research: Planets, v. 125, no. e2019JE005975, https://doi.org/10.1029/2019JE005975.

Hammond, W.C., Blewitt, G., and Kreemer, C., 2014, Steady contemporary deformation in the central Basin and Range Province, western United States: Journal of Geophysical Research: Solid Earth, v. 119, p. 5235–5253, https://doi.org/10.1002/2014JB011145.

Heizler, M.T., Perry, F.V., Crowe, B.M., Peters, L., and Appelt, R., 1999, The age of the Lathrop Wells volcanic center: An $^{40}Ar/^{39}Ar$ dating investigation: Journal of Geophysical Research: Solid Earth, v. 104, p. 767–804, https://doi.org/10.1029/1998JB900002.

Hildreth, W., Fierstein, J., Champion, D., and Calvert, A., 2014, Mammoth Mountain and its mafic periphery—A late Quaternary volcanic field in eastern California: Geosphere, v. 10, p. 1315–1365, https://doi.org/10.1130/GES01053.1.

Hintze, L.F., Davis, F.D., Rowley, P.D., Cunningham, C.G., Steven, T.A., and Willis, G.C., 2003, Geologic map of the Richfield 30′ × 60′ quadrangle, southeast Millard County and parts of Beaver, Piute, and Sevier Counties: Utah Geological Survey Map 195, scale 1:100,000, 2 plates.

Ho, C.-H., and Smith, E.I., 1998, A spatial-temporal/3-D model for volcanic hazard assessment: Application to the Yucca Mountain region, Nevada: Mathematical Geology, v. 30, p. 497–510, https://doi.org/10.1023/A:1021785910495.

Holm, R.F., 1987, Significance of agglutinate mounds on lava flows associated with monogenetic cones: An example at Sunset Crater, northern Arizona: Geological Society of America Bulletin, v. 99, p. 319–324, https://doi.org/10.1130/0016-7606(1987)99<319:SOAMOL>2.0.CO;2.

Holm, R.F., 1988, Geologic map of San Francisco, Elden Mountain, and Dry Lake Hills, Coconino County, Arizona: U.S. Geological Survey Miscellaneous Investigations Map 1–1663, scale 1:24,000, 1 sheet, 12 p. text.

Holtzman, B.K., and Kohlstedt, D.L., 2007, Stress-driven melt segregation and strain partitioning in partially molten rocks: Effects of stress and strain: Journal of Petrology, v. 48, p. 2379–2406, https://doi.org/10.1093/petrology/egm065.

Hooper, D.M., and Sheridan, M.F., 1998, Computer-simulation models of scoria cone degradation: Journal of Volcanology and Geothermal Research, v. 83, p. 241–267, https://doi.org/10.1016/S0377-0273(98)00031-6.

Johnson, P.J., Valentine, G.A., Cortés, J.A., and Tadini, A., 2014, Basaltic tephra from monogenetic Marcath Volcano, central Nevada: Journal of Volcanology and Geothermal Research, v. 281, p. 27–33, https://doi.org/10.1016/j.jvolgeores.2014.05.007.

Karlstrom, K.E., Crow, R.S., Peters, L., McIntosh, W.C., Raucci, J., Crossey, L.J., Umhoefer, P., and Dunbar, N., 2007, $^{40}Ar/^{39}Ar$ and field studies of Quaternary basalts in Grand Canyon and model for carving Grand Canyon: Quantifying the interaction of river incision and normal faulting across the western edge of the Colorado Plateau: Geological Society of America Bulletin, v. 119, p. 1283–1312, https://doi.org/10.1130/0016-7606(2007)119[1283:AAFSOQ]2.0.CO;2.

Katz, R.F., Spiegelman, M., and Holtzman, B., 2006, The dynamics of melt and shear localization in partially molten aggregates: Nature, v. 442, p. 676–679, https://doi.org/10.1038/nature05039.

Kelley, S.A., McIntosh, W.C., Goff, F., Kempter, K.A., Wolff, J.A., Esser, R., Braschayko, S., Love, D., and Gardner, J.N., 2013, Spatial and temporal trends in pre-caldera Jemez Mountains volcanic and fault activity: Geosphere, v. 9, p. 614–646, https://doi.org/10.1130/GES00897.1.

Kempton, P.D., and Dungan, M.A., 1989, Geology and petrology of basalts and included mafic, ultramafic, and granulitic xenoliths of the Geronimo Volcanic Field, southeastern Arizona, *in* Chapin, C.E., and Zidek, J., eds., Field Excursions to Volcanic Terranes in the Western United States, Volume I: Southern Rocky Mountain Region: Santa Fe, New Mexico, USA, New Mexico Bureau of Mines and Mineral Resources Memoir 46, p. 161–173.

Kempton, P.D., Dungan, M.A., and Blanchard, D.P., 1987, Petrology and geochemistry of xenolith-bearing alkalic basalts from the Geronimo Volcanic Field, southeast Arizona: Evidence for polybaric fractionation and implications for mantle heterogeneity, *in* Morris, E.M., and Pasteris, J.D., eds., Mantle Metasomatism and Alkaline Magmatism: Geological Society of America Special Paper 215, p. 347–370, https://doi.org/10.1130/SPE215-p347.

Kempton, P.D., Harmon, R.S., Hawkesworth, C.J., and Moorbath, S., 1990, Petrology and geochemistry of lower crustal granulites from the Geronimo Volcanic Field, southeastern Arizona: Geochimica et Cosmochimica Acta, v. 54, p. 3401-3426, https://doi.org/10.1016/0016-7037(90)90294-U.

Kumar, P., Kind, R., Yuan, X., and Mechie, J., 2012, USArray receiver function images of the lithosphere-asthenosphere boundary: Seismological Research Letters, v. 83, p. 486–491, https://doi.org/10.1785/gssrl.83.3.486.

Levander, A., Schmandt, B., Miller, M.S., Liu, K., Karlstrom, K.E., Crow, R.S., Lee, C.-T.A., and Humphreys, E.D., 2011, Continuing Colorado plateau uplift by delamination-style convective lithospheric downwelling: Nature, v. 472, p. 461–465, https://doi.org/10.1038/nature10001.

Luhr, J.F., and Simkin, T., eds., 1993, Parícutin, the Volcano Born in a Mexican Cornfield: Phoenix, Arizona, USA, Geoscience Press, Inc., 427 p.

Lutz, T.M., and Gutmann, J.T., 1995, An improved method for determining and characterizing alignments of pointlike features and its implications for the Pinacate volcanic field, Sonora, Mexico: Journal of Geophysical Research: Solid Earth, v. 100, p. 17659–17670, https://doi.org/10.1029/95JB01058.

Lynch, D.J., 1981, Genesis and geochronology of alkaline volcanism in the Pinacate volcanic field, northwestern Sonora, Mexico [Ph.D. thesis]: Tucson, Arizona, USA, University of Arizona, 248 p.

Lynch, D.J., Musselman, T.E., Gutmann, J.T., and Patchett, P.J., 1993, Isotopic evidence for the origin of Cenozoic volcanic rocks in the Pinacate volcanic field, northwestern Mexico: Lithos, v. 29, p. 295–302, https://doi.org/10.1016/0024-4937(93)90023-6.

Marzocchi, W., and Bebbington, M.S., 2012, Probabilistic eruption forecasting at short and long time scales: Bulletin of Volcanology, v. 74, p. 1777–1805, https://doi.org/10.1007/s00445-012-0633-x.

McGee, L.E., and Smith, I.E.M., 2016, Interpreting chemical compositions of small scale basaltic systems: A review: Journal of Volcanology and Geothermal Research, v. 325, p. 45–60, https://doi.org/10.1016/j.jvolgeores.2016.06.007.

McGee, L.E., Millet, M.-A., Smith, I.E.M., Németh, K., and Lindsay, J.M., 2012, The inception and progression of melting in a monogenetic eruption: Motukorea Volcano, the Auckland Volcanic Field, New Zealand: Lithos, v. 155, p. 360–374, https://doi.org/10.1016/j.lithos.2012.09.012.

McNutt, S.R., and Roman, D.C., 2015, Volcano seismicity, *in* Sigurdsson, H., Houghton, B., McNutt, S.R., Rymer, H., and Stix, J., eds, The Encyclopedia of Volcanoes: Amsterdam, Elsevier, p. 1011–1034, https://doi.org/10.1016/B978-0-12-385938-9.00059-6.

Mnich, M.E., 2019, Petrogenesis of basaltic lavas in Iceland and the Springerville volcanic field, U.S.A.: The influence of tectonic setting, depth of melting, and volatiles [Ph.D. thesis]: Amherst, Massachusetts, USA, University of Massachusetts, 184 p.

Mnich, M.E., and Condit, C.D., 2018, Basaltic magmatic mapping: A suggested methodology and the resulting petrologic and volcanic hazard implications from the Springerville Volcanic Field, east central Arizona: Journal of Volcanology and Geothermal Research, v. 366, p. 58–73, https://doi.org/10.1016/j.jvolgeores.2018.09.009.

Moore, R.B., and Wolfe, E.W., 1987, Geologic map of the east part of the San Francisco volcanic field, north-central Arizona: U.S. Geological Survey Map MF-1960, scale 1:50,000, 2 sheets, 46 p. text.
Morgan, P., Sass, J.H., Duffield, W., Felger, T., Fry, B.N., and Peters, L., 2004, Geothermal resource evaluation program of the Eastern San Francisco Volcanic Field, Arizona: U.S. Department of Energy, Project GRED II Final Report, Agreement # DE-FC04–2002AL68298, 58 p.
Muirhead, J.D., Van Eaton, A.R., Re, G., White, J.D.L., and Ort, M.H., 2016, Monogenetic volcanoes fed by interconnected dikes and sills in the Hopi Buttes volcanic field, Navajo Nation, USA: Bulletin of Volcanology, v. 78, p. 11, https://doi.org/10.1007/s00445-016-1005-8.
Nereson, A., Stroud, J., Karlstrom, K., Heizler, M., and McIntosh, W., 2013, Dynamic topography of the western Great Plains: Geomorphic and $^{40}Ar/^{39}Ar$ evidence for mantle-driven uplift associated with the Jemez lineament of NE New Mexico and SE Colorado: Geosphere, v. 9, p. 521–545, https://doi.org/10.1130/GES00837.1.
Newhall, C.G., Ulrich, G.E., and Wolfe, E.W., 1987, Geologic map of the southwest part of the San Francisco volcanic field, north-central Arizona: U.S. Geological Survey Miscellaneous Field Studies Map MF-1958, scale 1:50 000, 2 sheets, 58 p. text.
Ort, M.H., Elson, M.D., Anderson, K.C., Duffield, W.A., Hooten, J.A., Champion, D.E., and Waring, G., 2008a, Effects of scoria-cone eruptions upon nearby human communities: Geological Society of America Bulletin, v. 120, p. 476–486, https://doi.org/10.1130/B26061.1.
Ort, M.H., Elson, M.D., Anderson, K.C., Duffield, W.A., and Samples, T.L., 2008b, Variable effects of cinder-cone eruptions on prehistoric agrarian human populations in the American southwest: Journal of Volcanology and Geothermal Research, v. 176, p. 363–376, https://doi.org/10.1016/j.jvolgeores.2008.01.031.
Parsons, T., 2006, The Basin and Range Province, *in* Olsen, K., ed., Continental Rifts: Evolution, Structure and Tectonics: Amsterdam, Elsevier, p. 277–324, https://doi.org/10.1016/S0419-0254(06)80015-7.
Passarelli, L., and Brodsky, E.E., 2012, The correlation between run-up and repose times of volcanic eruptions: Geophysical Journal International, v. 188, p. 1025–1045, https://doi.org/10.1111/j.1365-246X.2011.05298.x.
Perry, F.V., Baldridge, W.S., and DePaolo, D.J., 1988, Chemical and isotopic evidence for lithospheric thinning beneath the Rio Grande rift: Nature, v. 332, p. 432–434, https://doi.org/10.1038/332432a0.
Perry, F.V., Baldridge, W.S., and DePaolo, D.J., 1990, Evolution of a magmatic system during continental extension: The Mount Taylor volcanic field, New Mexico: Journal of Geophysical Research: Solid Earth, v. 95, p. 19327–19348, https://doi.org/10.1029/JB095iB12p19327.
Plank, T., and Forsyth, D.W., 2016, Thermal structure and melting conditions in the mantle beneath the Basin and Range province from seismology and petrology: Geochemistry, Geophysics, Geosystems, v. 17, p. 1312–1338, https://doi.org/10.1002/2015GC006205.
Poblete Piedrabuena, M.Á., Martí Molist, J., Bergua, S.B., and Marino Alfonso, J.L., 2019, Geomorphological evolution and chronology of the eruptive activity of the Columba and Cuevas volcanoes (Campo de Calatrava Volcanic Field, Ciudad Real, Central Spain): Geomorphology, v. 336, p. 52–64, https://doi.org/10.1016/j.geomorph.2019.03.026.
Putirka, K.D., and Busby, C.J., 2011, Introduction: Origin and evolution of the Sierra Nevada and Walker Lane: Geosphere, v. 7, p. 1269–1272, https://doi.org/10.1130/GES00761.1.
Rasoazanamparany, C., Widom, E., Valentine, G.A., Smith, E.I., Cortés, J.A., Kuentz, D., and Johnsen, R., 2015, Origin of chemical and isotopic heterogeneity in a mafic, monogenetic volcanic Field: A case study of the Lunar Crater Volcanic Field, Nevada: Chemical Geology, v. 397, p. 76–93, https://doi.org/10.1016/j.chemgeo.2015.01.004.
Re, G., White, J.D.L., and Ort, M.H., 2015, Dikes, sills, and stress-regime evolution during emplacement of the Jagged Rocks Complex, Hopi Buttes Volcanic Field, Navajo Nation, USA: Journal of Volcanology and Geothermal Research, v. 295, p. 65–79, https://doi.org/10.1016/j.jvolgeores.2015.01.009.
Reid, M.R., Bouchet, R.A., Blichert-Toft, J., Levander, A., Liu, K., Miller, M.S., and Ramos, F.C., 2012, Melting under the Colorado Plateau, USA: Geology, v. 40, p. 387–390, https://doi.org/10.1130/G32619.1.
Richardson, J.A., Connor, C.B., Wetmore, P.H., Connor, L.J., and Gallant, E.A., 2015, Role of sills in the development of volcanic fields: Insights from lidar mapping surveys of the San Rafael Swell, Utah: Geology, v. 43, p. 1023–1026, https://doi.org/10.1130/G37094.1.
Riggs, N.R., and Duffield, W.A., 2008, Record of complex scoria cone activity at Red Mountain, Arizona, USA, and implications for monogenetic mafic volcanoes: Journal of Volcanology and Geothermal Research, v. 178, p. 763–776, https://doi.org/10.1016/j.jvolgeores.2008.09.004.
Rivera, T.A., White, C.M., Schmitz, M.D., and Jicha, B.R., 2021, Petrogenesis of Pleistocene basalts from the Western Snake River Plain, Idaho: Journal of Petrology, v. 62, no. egaa108, https://doi.org/10.1093/petrology/egaa108.
Rowley, P.D., Vice, G.S., McDonald, R.E., Anderson, J.J., Machette, M.N., Maxwell, D.J., Ekren, B., Cunningham, C.G., Steven, T.A., and Wardlaw, B.R., 2005, Interim geologic map of the Beaver 30′ × 60′ quadrangle, Beaver, Piute, Iron, and Garfield Counties, Utah: Utah Geological Survey Open-File Report 454, scale 1:100,000, 1 sheet, 27 p. text.
Rowley, P.D., Williams, V.S., Vice, G.S., Maxwell, D.J., Hacker, D.B., Snee, L.W., and Mackin, J.J., 2006, Interim geologic map of the Cedar City 30′ × 60′ quadrangle, Iron and Washington Counties, Utah: Utah Geological Survey Open-File Report 476DM, scale 1:100,000, 2 sheets.
Roy, M., Jordan, T.H., and Pederson, J., 2009, Colorado Plateau magmatism and uplift by warming of heterogeneous lithosphere: Nature, v. 459, p. 978–982, https://doi.org/10.1038/nature08052.
Roy, M., Gold, S., Johnson, A., Osuna Orozco, R., Holtzman, B.K., and Gaherty, J., 2016, Macroscopic coupling of deformation and melt migration at continental interiors, with applications to the Colorado Plateau: Journal of Geophysical Research: Solid Earth, v. 121, p. 3762–3781, https://doi.org/10.1002/2015JB012149.
Rudzitis, S., Reid, M.R., and Blichert-Toft, J., 2016, On edge melting under the Colorado Plateau margin: Geochemistry, Geophysics, Geosystems, v. 17, p. 2835–2854, https://doi.org/10.1002/2016GC006349.
Schmitt, A.K., and Hulen, J.B., 2008, Buried rhyolites within the active, high-temperature Salton Sea geothermal system: Journal of Volcanology and Geothermal Research, v. 178, p. 708–718, https://doi.org/10.1016/j.jvolgeores.2008.09.001.
Schulte-Pelkum, V., Biasi, G., Sheehan, A., and Jones, C., 2011, Differential motion between upper crust and lithospheric mantle in the central Basin and Range: Nature Geoscience, v. 4, p. 619–623, https://doi.org/10.1038/ngeo1229.
Self, S., Goff, F., Gardner, J.N., Wright, J.V., and Kite, W.M., 1986, Explosive rhyolitic volcanism in the Jemez Mountains: Vent locations, caldera development and relation to regional structure: Journal of Geophysical Research: Solid Earth, v. 91, p. 1779–1798, https://doi.org/10.1029/JB091iB02p01779.
Shen, W., Ritzwoller, M.H., and Schulte-Pelkum, V., 2013, A 3-D model of the crust and uppermost mantle beneath the Central and Western US by joint inversion of receiver functions and surface wave dispersion: Journal of Geophysical Research: Solid Earth, v. 118, p. 262–276, https://doi.org/10.1029/2012JB009602.
Shepard, M.K., Arvidson, R.E., Caffee, M., Finkel, R., and Harris, L., 1995, Cosmogenic exposure ages of basaltic flows: Lunar Crater volcanic field, Nevada: Geology, v. 23, p. 21–24, https://doi.org/10.1130/0091-7613(1995)023<0021:CEAOBF>2.3.CO;2.
Sheridan, M.F., and Updike, R.G., 1975, Sugarloaf Mountain Tephra—A Pleistocene rhyolitic deposit of base-surge origin in northern Arizona: Geological Society of America Bulletin, v. 86, p. 571–581, https://doi.org/10.1130/0016-7606(1975)86<571:SMTAPR>2.0.CO;2.
Singleton, J.S., Seymour, N.M., Reynolds, S.J., Vomocil, T., and Wong, M.S., 2019, Distributed Neogene faulting across the western to central Arizona metamorphic core complex belt: Syn-extensional constriction and superposition of the Pacific-North America plate boundary on the southern Basin and Range: Geosphere, v. 15, p. 1409–1435, https://doi.org/10.1130/GES02036.1.
Smith, E.I., Sánchez, A., Walker, J.D., and Wang, K., 1999, Geochemistry of mafic magmas in the Hurricane volcanic field, Utah: Implications for small- and large-scale chemical variability of the lithospheric mantle: The Journal of Geology, v. 107, p. 433–448, https://doi.org/10.1086/314355.
Smith, I.E.M., and Németh, K., 2017, Source to surface model of monogenetic volcanism: A critical review, *in* Németh, K., Carrasco-Nuñez, G., Aranda-Gómez, J.J., and Smith, I.E.M., eds., Monogenetic Volcanism: Geological Society, London, Special Publication 446, p. 1–28, https://doi.org/10.1144/SP446.14.
Smith, R.L., and Luedke, R.G., 1984, Potentially active volcanic lineaments and loci in western conterminous United States, *in* Explosive Volcanism: Inception, Evolution, and Hazards: Studies in Geophysics: Washington, D.C., National Academy Press, p. 47–66.
Soldati, A., Beem, J., Gomez, F., Huntley, J.W., Robertson, T., and Whittington, A., 2017, Emplacement dynamics and timescales of a Holocene flow from the Cima Volcanic Field (CA): Insights from rheology and morphology: Journal of Volcanology and Geothermal Research, v. 347, p. 91–111, https://doi.org/10.1016/j.jvolgeores.2017.09.005.
Sonder, L.J., and Jones, C.H., 1999, Western United States extension: How the West was widened: Annual Review of Earth and Planetary Sciences, v. 27, p. 417–462, https://doi.org/10.1146/annurev.earth.27.1.417.
Sweeney, M.R., Grosso, Z.S., and Valentine, G.A., 2018, Topographic controls on a phreatomagmatic maar-diatreme eruption: Field and numerical results from the Holocene Dotsero volcano (Colorado, USA): Bulletin of Volcanology, v. 80, p. 78, https://doi.org/10.1007/s00445-018-1253-x.
Tadini, A., Bonali, F.L., Corazzato, C., Cortés, J.A., Tibaldi, A., and Valentine, G.A., 2014, Spatial distribution and structural analysis of vents in the Lunar Crater Volcanic Field (Nevada, USA): Bulletin of Volcanology, v. 76, no. 11, https://doi.org/10.1007/s00445-014-0877-8.

Tanaka, K.L., Shoemaker, E.M., Ulrich, G.E., and Wolfe, E.W., 1986, Migration of volcanism in the San Francisco volcanic field, Arizona: Geological Society of America Bulletin, v. 97, p. 129–141, https://doi.org/10.1130/0016-7606(1986)97<129:MOVITS>2.0.CO;2.

Thompson, R.N., Ottley, C.J., Smith, P.A., Pearson, D.G., Dickin, A.P., Morrison, M.A., Leat, P.T., and Gibson, S.A., 2005, Source of the Quaternary alkalic basalts, picrites and basanites of the Potrillo Volcanic Field, New Mexico, USA: Lithosphere or convecting mantle?: Journal of Petrology, v. 46, p. 1603–1643, https://doi.org/10.1093/petrology/egi028.

Ulrich, G.E., and Bailey, N.G., 1987, Geologic map of the SP Mountain part of the San Francisco volcanic field, north-central Arizona: U.S. Geological Survey Miscellaneous Field Studies Map MF-1956, scale 1:50 000, 2 sheets.

Valentine, G.A., and Connor, C.B., 2015, Basaltic volcanic fields, *in* Sigurdsson, H., Houghton, B., McNutt, S.R., Rymer, H., and Stix, J., eds., The Encyclopedia of Volcanoes (2nd Edition): Amsterdam, Elsevier, p. 423–439, https://doi.org/10.1016/B978-0-12-385938-9.00023-7.

Valentine, G.A., and Cortés, J.A., 2013, Time and space variations in magmatic and phreatomagmatic eruptive processes at Easy Chair (Lunar Crater Volcanic Field, Nevada, USA): Bulletin of Volcanology, v. 75, no. 9, https://doi.org/10.1007/s00445-013-0752-z.

Valentine, G.A., and Gregg, T.K.P., 2008, Continental basaltic volcanoes—processes and problems: Journal of Volcanology and Geothermal Research, v. 177, p. 857–873, https://doi.org/10.1016/j.jvolgeores.2008.01.050.

Valentine, G.A., and Hirano, N., 2010, Mechanisms for low-flux intraplate volcanic fields—Basin and Range (North America) and northwest Pacific Ocean: Geology, v. 38, p. 55–58, https://doi.org/10.1130/G30427.1.

Valentine, G.A., and Krogh, K.E.C., 2006, Emplacement of shallow dikes and sills beneath a small basaltic volcanic center—the role of pre-existing structure (Paiute Ridge, southern Nevada, USA): Earth and Planetary Science Letters, v. 246, p. 217–230, https://doi.org/10.1016/j.epsl.2006.04.031.

Valentine, G.A., and Perry, F.V., 2007, Tectonically controlled, time-predictable basaltic volcanism from a lithospheric mantle source (central Basin and Range Province, USA): Earth and Planetary Science Letters, v. 261, p. 201–216, https://doi.org/10.1016/j.epsl.2007.06.029.

Valentine, G.A., and Perry, F.V., 2009, Volcanic risk assessment at Yucca Mountain, NV, USA: Integration of geophysics, geology, and modeling, *in* Connor, C., Connor, L., and Chapman, N., eds., Volcanism, Tectonism, and Siting Nuclear Facilities: Cambridge, UK, Cambridge University Press, p. 452–480, https://doi.org/10.1017/CBO9780511635380.020.

Valentine, G.A., and White, J.D.L., 2012, Revised conceptual model for maar-diatremes: Subsurface processes, energetics, and eruptive products: Geology, v. 40, p. 1111–1114, https://doi.org/10.1130/G33411.1.

Valentine, G.A., Perry, F.V., Krier, D., Keating, G.N., Kelley, R.E., and Cogbill, A.H., 2006, Small-volume basaltic volcanoes: Eruptive products and processes, and post-eruptive geomorphic evolution in Crater Flat (Pleistocene), southern Nevada: Geological Society of America Bulletin, v. 118, p. 1313–1330, https://doi.org/10.1130/B25956.1.

Valentine, G.A., Krier, D.J., Perry, F.V., and Heiken, G., 2007, Eruptive and geomorphic processes at the Lathrop Wells scoria cone volcano: Journal of Volcanology and Geothermal Research, v. 161, p. 57–80, https://doi.org/10.1016/j.jvolgeores.2006.11.003.

Valentine, G.A., Shufelt, N.L., and Hintz, A.R.L., 2011, Models of maar volcanoes, Lunar Crater (Nevada, USA): Bulletin of Volcanology, v. 73, p. 753–765, https://doi.org/10.1007/s00445-011-0451-6.

Valentine, G.A., Cortés, J.A., Widom, E., Smith, E.I., Rasoazanamparany, C., Johnsen, R., Briner, J.P., Harp, A.G., and Turrin, B., 2017, Lunar Crater volcanic field (Reveille and Pancake Ranges, Basin and Range Province, Nevada, USA): Geosphere, v. 13, p. 391–438, https://doi.org/10.1130/GES01428.1.

van Otterloo, J., Raveggi, M., Cas, R.A.F., and Maas, R., 2014, Polymagmatic activity at the monogenetic Mt. Gambier Volcanic Complex in the Newer Volcanics Province, SE Australia: New insights into the occurrence of intraplate volcanic activity in Australia: Journal of Petrology, v. 55, p. 1317–1351, https://doi.org/10.1093/petrology/egu026.

van Wijk, J.W., Baldridge, W.S., van Hunen, J., Goes, S., Aster, R., Coblentz, D.D., Grand, S.P., and Ni, J., 2010, Small-scale convection at the edge of the Colorado Plateau: Implications for topography, magmatism, and evolution of Proterozoic lithosphere: Geology, v. 38, p. 611–614, https://doi.org/10.1130/G31031.1.

Varley, N., Johnson, J., Ruiz, M., Reyes, G., and Martin, K., 2006, Applying statistical analysis to understanding the dynamics of volcanic explosions, *in* Mader, H.M., Coles, S.G., Connor, C.B., and Connor, L.J., eds., Statistics in Volcanology: Geological Society, London, Special Publication of the International Association of Volcanology and Chemistry of the Earth's Interior 1, p. 57–76.

Wehrmann, H., and Dzierma, Y., 2011, Applicability of statistical analysis to the geological record of Villarrica and Lanín volcanoes, Southern Volcanic Zone, Chile: Journal of Volcanology and Geothermal Research, v. 200, p. 99–115, https://doi.org/10.1016/j.jvolgeores.2010.11.009.

Wells, S.G., Dohrenwend, J.C., McFadden, L.D., Turrin, B.D., and Mahrer, K.D., 1985, Late Cenozoic landscape evolution on lava flow surfaces of the Cima volcanic field, Mojave Desert, California: Geological Society of America Bulletin, v. 96, p. 1518–1529, https://doi.org/10.1130/0016-7606(1985)96<1518:LCLEOL>2.0.CO;2.

Wells, S.G., McFadden, L.D., Renault, C.E., and Crowe, B.M., 1990, Geomorphic assessment of late Quaternary volcanism in the Yucca Mountain area, southern Nevada: Implications for the proposed high-level radioactive waste repository: Geology, v. 18, p. 549–553, https://doi.org/10.1130/0091-7613(1990)018<0549:GAOLQV>2.3.CO;2.

Wenger, E., Büchner, J., Tietz, O., and Mrlina, J., 2017, The polycyclic Lausche Volcano (Lausitz Volcanic Field) and its message concerning landscape evolution in the Lausitz Mountains (northern Bohemian Massif, Central Europe): Geomorphology, v. 292, p. 193–210, https://doi.org/10.1016/j.geomorph.2017.04.021.

Wesnousky, S.G., 2005, The San Andreas and Walker Lane fault systems, western North America: Transpressional, transtensional, cumulative slip, and the structural evolution of a major transform plate boundary: Journal of Structural Geology, v. 27, p. 1505–1512, https://doi.org/10.1016/j.jsg.2005.01.015.

White, J.D.L., 2001, Eruption and reshaping of Pahvant Butte volcano in Pleistocene Lake Bonneville, *in* White, J.D.L., and Riggs, N.R., eds., Volcaniclastic Sedimentation in Lacustrine Settings: International Association of Sedimentologists Special Publication 30, p. 61–80, https://doi.org/10.1002/9781444304251.ch4.

White, J.D.L., and Ross, P.S., 2011, Maar-diatreme volcanoes: A review: Journal of Volcanology and Geothermal Research, v. 201, no. 1–4, p. 1–29, https://doi.org/10.1016/j.jvolgeores.2011.01.010.

Wohletz, K.H., and Sheridan, M.F., 1979, A model of pyroclastic surge, *in* Chapin, C.E., and Elston, W.E., Ash Flow Tuffs: Geological Society of America Special Paper 180, p. 177–194, https://doi.org/10.1130/SPE180-p177.

Wohletz, K.H., and Sheridan, M.F., 1983, Hydrovolcanic explosions II. Evolution of basaltic tuff rings and tuff cones: American Journal of Science, v. 283, p. 385–413, https://doi.org/10.2475/ajs.283.5.385.

Wolfe, E.W., Ulrich, G.E., Holm, R.F., Moore, R.B., and Newhall, C.G., 1987a, Geologic map of the central part of the San Francisco volcanic field, north-central Arizona: U.S. Geological Survey Miscellaneous Field Studies Map MF-1959, scale 1:50 000, 2 sheets, 86 p. text.

Wolfe, E.W., Ulrich, G.E., and Newhall, C.G., 1987b, Geologic map of the northwest part of the San Francisco volcanic field, north-central Arizona: U.S. Geological Survey Miscellaneous Field Studies Map MF-1957, scale 1:50,000, 2 sheets.

Wolff, J.A., Heikoop, C.E., and Ellisor, R., 2000, Hybrid origin of Rio Grande rift hawaiites: Geology, v. 28, p. 203–206, https://doi.org/10.1130/0091-7613(2000)28<203:HOORGR>2.0.CO;2.

Wolff, J.A., Rowe, M.C., Teasdale, R., Gardner, J.N., Ramos, F.C., and Heikoop, C.E., 2005, Petrogenesis of pre-caldera mafic lavas, Jemez Mountains volcanic field (New Mexico, USA): Journal of Petrology, v. 46, p. 407–439, https://doi.org/10.1093/petrology/egh082.

Wood, C.A., 1980, Morphometric analysis of cinder cone degradation: Journal of Volcanology and Geothermal Research, v. 8, p. 137–160, https://doi.org/10.1016/0377-0273(80)90101-8.

Wood, C.A., and Kienle, J., 1990, Volcanoes of North America: Cambridge, UK, Cambridge University Press, 354 p.

Younger, Z.P., Valentine, G.A., and Gregg, T.K.P., 2019, 'A'ā lava emplacement and the significance of rafted pyroclastic material: Marcath volcano (Nevada, USA): Bulletin of Volcanology, v. 81, p. 50, https://doi.org/10.1007/s00445-019-1309-6.

Zawacki, E.E., Clarke, A.B., Arrowsmith, J.R., Bonadonna, C., and Lynch, D.J., 2019, Tecolote volcano, Pinacate volcanic field (Sonora, Mexico): A case of highly explosive basaltic volcanism and shifting eruptive styles: Journal of Volcanology and Geothermal Research, v. 379, p. 23–44, https://doi.org/10.1016/j.jvolgeores.2019.04.011.

Zimbelman, J.R., and Johnston, A.K., 2001, Improved topography of the Carrizozo lava flow: Implications for emplacement conditions: New Mexico Museum of Natural History and Science Bulletin, v. 18, p. 131–136.